Journal of Computational and Applied Mathematics 436 (2024) 115409

Contents lists available at ScienceDirect

Journal of Computational and Applied Mathematics

journal homepage: www.elsevier.com/locate/cam

Convergence analysis of a temporally second-order accurate finite element scheme for the Cahn–Hilliard-Magnetohydrodynamics system of equations

Cheng Wang [a], Jilu Wang [b], Steven M. Wise [c], Zeyu Xia [b], Liwei Xu [d,*]

[a] *Mathematics Department, University of Massachusetts, North Dartmouth, MA 02747, USA*
[b] *School of Science, Harbin Institute of Technology, Shenzhen 518055, China*
[c] *Department of Mathematics, The University of Tennessee, Knoxville, TN 37996, USA*
[d] *School of Mathematical Sciences, University of Electronic Science and Technology of China, Sichuan, 611731, China*

A R T I C L E I N F O

Article history:
Received 3 November 2022
Received in revised form 11 April 2023

Keywords:
CH-MHD system
Crank–Nicolson method
Finite element approximation
Unique solvability
Unconditional energy stability
Error estimates

A B S T R A C T

In this paper we propose and analyze a temporally second-order accurate numerical scheme for the Cahn–Hilliard-Magnetohydrodynamics system of equations. The scheme is based on a modified Crank–Nicolson-type approximation for the time discretization and a mixed finite element method for the spatial discretization. The modified Crank–Nicolson approximation enables us to carry out the mass conservation and the energy stability analysis. Error estimates are derived for the phase field in the $L^\infty_\tau(0,T;H^1)$ norm, and for the velocity and the magnetic fields in the $L^\infty_\tau(0,T;L^2)$ norm, respectively. Numerical examples are presented to validate the theoretical results of the proposed scheme.

1. Introduction

In this paper, we consider a two-phase incompressible fluid, where the phases interact through a magnetic field. The physical system is modeled by a diffuse interface framework and is formulated as follows [1]:

$$\partial_t\phi + \nabla\cdot(\phi\boldsymbol{u}) = \varepsilon\nabla\cdot(M(\phi)\nabla w), \tag{1}$$

$$\varepsilon^{-1}(\phi^3-\phi) - \varepsilon\Delta\phi = w, \tag{2}$$

$$\rho(\partial_t\boldsymbol{u} + (\boldsymbol{u}\cdot\nabla)\boldsymbol{u}) - \nabla\cdot(\eta(\phi)\nabla\boldsymbol{u}) + \nabla p + \lambda\phi\nabla w = \mu(\nabla\times\boldsymbol{B})\times\boldsymbol{B}, \tag{3}$$

$$\partial_t\boldsymbol{B} + \mu^{-1}\nabla\times(\sigma(\phi)^{-1}\nabla\times\boldsymbol{B}) - \nabla\times(\boldsymbol{u}\times\boldsymbol{B}) = 0, \tag{4}$$

$$\nabla\cdot\boldsymbol{u} = 0, \tag{5}$$

over $\Omega\times[0,T]$, where Ω is a bounded and convex polyhedral domain in $\mathbb{R}^3$ (or polygonal domain in $\mathbb{R}^2$), and T stands for the final time. The above system is known as the Cahn–Hilliard-Magnetohydrodynamic (CH-MHD) model. In the above equations, the unknown $\boldsymbol{u}$ denotes the velocity vector; $\boldsymbol{B}$, the magnetic field; p, the pressure; ϕ, the phase field; and w, the chemical potential. The constant μ is the magnetic permeability, and $\varepsilon > 0$ represents the interfacial width between

* Corresponding author.
E-mail addresses: cwang1@umassd.edu (C. Wang), wangjilu@hit.edu.cn (J. Wang), swise1@utk.edu (S.M. Wise), xiazeyu@hit.edu.cn (Z. Xia), xul@uestc.edu.cn (L. Xu).

https://doi.org/10.1016/j.cam.2023.115409
0377-0427/

two phases. The coefficient ρ is a positive constant representing the fluid density, and we set it to be 1 for brevity. The parameters $\eta(\phi)$ and $\sigma(\phi)$ stand for the hydrodynamic viscosity and electric conductivity, respectively, which are assumed to satisfy

$$0 < \underline{\eta} := \min(\eta_1, \eta_2) \le \eta(\phi) \le \max(\eta_1, \eta_2) =: \overline{\eta},$$
$$0 < \underline{\sigma} := \min(\sigma_1, \sigma_2) \le \sigma(\phi) \le \max(\sigma_1, \sigma_2) =: \overline{\sigma},$$

where η_i and σ_i $(i = 1, 2)$ denote the viscosity and electric conductivity of the pure phase fluid i. It is assumed that $\eta(\phi)$ and $\sigma(\phi)^{-1}$ are Lipschitz continuous functions with respect to ϕ. Specific expressions of functions $\eta(\phi)$ and $\sigma(\phi)$ can be found in [1]. For the sake of simplicity, we assume $\eta(\phi) \equiv \eta$ and $\sigma(\phi) \equiv \sigma$ in this paper, where η and σ are positive constants, for the sake of simplicity. Furthermore, the mobility function $M(\phi)$ is set to be 1. The term $\lambda\phi\nabla w$ represents the continuum surface tension force with λ being a positive constant [2,3].

With the assumptions mentioned above, we can simplify the system (1)–(5) as

$$\partial_t \phi + \nabla \cdot (\phi \boldsymbol{u}) = \varepsilon \Delta w, \tag{6}$$
$$\varepsilon^{-1}(\phi^3 - \phi) - \varepsilon \Delta \phi = w, \tag{7}$$
$$\partial_t \boldsymbol{u} + (\boldsymbol{u} \cdot \nabla)\boldsymbol{u} - \eta \Delta \boldsymbol{u} + \nabla p + \lambda \phi \nabla w = \mu (\nabla \times \boldsymbol{B}) \times \boldsymbol{B}, \tag{8}$$
$$\mu \partial_t \boldsymbol{B} + \sigma^{-1} \nabla \times (\nabla \times \boldsymbol{B}) - \mu \nabla \times (\boldsymbol{u} \times \boldsymbol{B}) = 0, \tag{9}$$
$$\nabla \cdot \boldsymbol{u} = 0. \tag{10}$$

The following boundary and initial conditions are used:

$$\frac{\partial \phi}{\partial \boldsymbol{n}} = \frac{\partial w}{\partial \boldsymbol{n}} = 0, \quad \boldsymbol{u} = 0, \quad \boldsymbol{B} \times \boldsymbol{n} = 0, \quad \text{on } \partial\Omega \times [0, T], \tag{11}$$
$$\phi|_{t=0} = \phi_0, \quad w|_{t=0} = w_0, \quad \boldsymbol{u}|_{t=0} = \boldsymbol{u}_0, \quad \boldsymbol{B}|_{t=0} = \boldsymbol{B}_0, \quad \text{in } \Omega, \tag{12}$$

where $\boldsymbol{n}$ denotes the outward unit normal vector on $\partial\Omega$. It is supposed that the initial condition $\nabla \cdot \boldsymbol{B}_0 = 0$, which implies $\nabla \cdot \boldsymbol{B}(\cdot, t) = 0$ for any $t > 0$.

In [1], Yang et al. proved the existence of weak solutions for the two-phase MHD system (1)–(5), and designed a temporally first-order accurate numerical scheme with mass-conservation, unique solvability, and unconditional energy stability. An abstract convergence result was also established. In [4], second-order linear schemes were proposed for solving the CH-MHD equations, based on the second-order backward differential formulation (BDF2) and Crank–Nicolson methods. In [5], Zhao et al. proposed and analyzed a linearized Crank–Nicolson scheme for the system (1)–(5), where the SAV method was used to deal with the nonlinear term in the Cahn–Hilliard equation. In [6], Su et al. proposed an efficient scheme to solve the CH-MHD model, where the IEQ method and projection method were applied to approximate the phase field equations and the MHD equations, respectively. The unconditional energy stabilities of the semi- and full-discrete schemes were also proved in [6]. In these previous works, error estimates of the fully discrete numerical schemes have not been available for the CH-MHD model.

The system (6)–(10) contains a challenging part, the incompressible MHD system, which describes the interaction between the fluid and the magnetic fields. This part has been widely applied in the engineering modeling, such as the plasma motion and the liquid-metal processing [7,8]. The incompressible MHD model is formulated as [9]

$$\mu \partial_t \boldsymbol{B} + \sigma^{-1} \nabla \times (\nabla \times \boldsymbol{B}) - \mu \nabla \times (\boldsymbol{u} \times \boldsymbol{B}) = 0, \tag{13}$$
$$\rho(\partial_t \boldsymbol{u} + \boldsymbol{u} \cdot \nabla \boldsymbol{u}) - \Delta \boldsymbol{u} + \nabla p - \mu (\nabla \times \boldsymbol{B}) \times \boldsymbol{B} = 0, \tag{14}$$
$$\nabla \cdot \boldsymbol{u} = 0. \tag{15}$$

There have been extensive works on regularity analysis for the continuous MHD system (13)–(15) [10–14]. In terms of numerical simulations, the $H^1(\Omega)$-conforming finite element methods (FEMs) have been widely adopted to approximate this system. Here, $d = 2, 3$, denotes the dimension of the domain. In [15], Gunzburger, Meir, and Peterson designed a numerical scheme based on $H^1(\Omega)$-conforming FEMs for the stationary MHD system. In [16], He proposed a first-order Euler semi-implicit scheme for solving the time-dependent MHD model, where the $H^1(\Omega)$-conforming FEM was used to approximate the magnetic field, and the convergence analysis of the scheme was considered. More developments on the $H^1(\Omega)$-conforming FEMs could be found in [17–22]. For the time-dependent MHD system, many existing works are dedicated to the study of temporally first-order accurate schemes, such as [16,23–25]. Recently, higher-order accurate temporal schemes have also attracted interest, in particular, BDF2-based methods in [26–28], and Crank–Nicolson-based methods in [29,30].

In addition to the fluid motion and the magnetic field evolution processes, another key feature in the physical system (6)–(10) is phase transition. The Allen–Cahn (AC) [31] and the Cahn–Hilliard (CH) [32] equations are fundamental gradient flow models in the description of the phase transition. Many numerical works have been reported [33–35], and the corresponding energy stability results have been proved. Neglecting the effect of magnetic fields, a combination of a phase field model and the Navier–Stokes equation [36,37], namely the Cahn–Hilliard–Navier–Stokes (CHNS) equations, has been proposed to describe some natural phenomena, such as two-phase flows with topological change, including pinch-off and droplet merging. Error estimates and energy stability analyses of various numerical methods for solving the CHNS system have been analyzed in [37–39]. In [37], Diegel et al. proposed a numerical scheme with finite element spatial discretization and a modified Crank–Nicolson method for the CHNS model and presented the analysis of unique solvability, mass conservation, unconditional energy stability, and error estimates. More related numerical works related to the models coupling with the phase fields can be found in [2,40–47] and the references therein.

In this paper we design a fully discrete numerical scheme, which combines the $H^1(\Omega)$-conforming FEM spatial discretization and a modified Crank–Nicolson temporal approximation, to solve the CH-MHD system (6)–(10). Precisely, a modified Crank–Nicolson discretization is applied to the nonlinear part associated with the double-well potential, which together with the Adams–Bashforth extrapolation to the concave term and a second-order convex splitting technique enables us to theoretically justify the unconditional energy stability of the numerical algorithm. Another modified Crank–Nicolson-type approximation is applied to the phase diffusion term. As a result, we can obtain the certain boundness of the numerical approximation for the phase field. With the above numerical design, we are able to prove the unique solvability, discrete mass conservation, unconditional energy stability, and error estimates for the proposed scheme.

This paper is organized as follows. In Section 2 we outline the variational formulation and derive the energy stability for the continuous system. The numerical scheme is constructed in Section 3, and the unique solvability, discrete mass-conservation, and energy stability of the scheme are established as well. The proof of error estimates is provided in Section 4. Several numerical examples and concluding remarks are presented in Sections 5 and 6, respectively.

2. Variational formulation and stability analysis

We adopt the conventional Sobolev spaces $W^{k,p}(\Omega)$, for $k \geq 0$ and $1 \leq p \leq \infty$, with the abbreviations $L^p(\Omega) = W^{0,p}(\Omega)$ and $H^k(\Omega) = W^{k,2}(\Omega)$, and define

$$H_0^1(\Omega) := \left\{ v \in H^1(\Omega) \mid v|_{\partial\Omega} = 0 \right\}, \quad L_0^2(\Omega) = \left\{ v \in L^2(\Omega) \;\middle|\; \int_\Omega v \, d\mathbf{x} = 0 \right\}.$$

The corresponding vector spaces are given by

$$\begin{aligned}
&\mathbf{L}^p(\Omega) = [L^p(\Omega)]^d, \quad \mathbf{W}^{k,p}(\Omega) = [W^{k,p}(\Omega)]^d, \\
&\mathbf{H}_0^1(\Omega) = [H_0^1(\Omega)]^d, \quad \mathring{\mathbf{H}}^1(\Omega) = \left\{ \boldsymbol{v} \in \mathbf{H}^1(\Omega) \mid \boldsymbol{v} \times \boldsymbol{n}|_{\partial\Omega} = 0 \right\},
\end{aligned}$$

where $d = 2, 3$, denotes the dimension of the domain Ω. In addition, the L^2 inner product is denoted by $(\cdot, \cdot)$.

The exact solution $(\phi, w, \boldsymbol{u}, \boldsymbol{B}, p)$ of (6)–(10) satisfies the following weak formulation: for almost all $t \in [0, T]$,

$$(\partial_t \phi, \xi) - (\phi \boldsymbol{u}, \nabla \xi) + \varepsilon(\nabla w, \nabla \xi) = 0, \tag{16}$$

$$\varepsilon^{-1}(\phi^3 - \phi, \varphi) + \varepsilon(\nabla \phi, \nabla \varphi) = (w, \varphi), \tag{17}$$

$$(\partial_t \boldsymbol{u}, \boldsymbol{v}) + b(\boldsymbol{u}, \boldsymbol{u}, \boldsymbol{v}) + \eta(\nabla \boldsymbol{u}, \nabla \boldsymbol{v}) - (p, \nabla \cdot \boldsymbol{v}) + \lambda(\phi \nabla w, \boldsymbol{v}) = \mu((\nabla \times \boldsymbol{B}) \times \boldsymbol{B}, \boldsymbol{v}), \tag{18}$$

$$\mu(\partial_t \boldsymbol{B}, \boldsymbol{l}) + \sigma^{-1}(\nabla \times \boldsymbol{B}, \nabla \times \boldsymbol{l}) - \mu(\boldsymbol{u} \times \boldsymbol{B}, \nabla \times \boldsymbol{l}) = 0, \tag{19}$$

$$(\nabla \cdot \boldsymbol{u}, q) = 0, \tag{20}$$

for any $(\xi, \varphi, \boldsymbol{v}, \boldsymbol{l}, q) \in (H^1(\Omega), H^1(\Omega), \mathbf{H}_0^1(\Omega), \mathring{\mathbf{H}}^1(\Omega), L^2(\Omega))$, where $b(\cdot, \cdot, \cdot)$ is defined by

$$b(\boldsymbol{u}, \boldsymbol{v}, \boldsymbol{w}) = \frac{1}{2}\left[(\boldsymbol{u} \cdot \nabla \boldsymbol{v}, \boldsymbol{w}) - (\boldsymbol{u} \cdot \nabla \boldsymbol{w}, \boldsymbol{v})\right], \quad \forall \boldsymbol{u}, \boldsymbol{v}, \boldsymbol{w} \in \mathbf{H}_0^1(\Omega). \tag{21}$$

Clearly, we have $b(\boldsymbol{u}, \boldsymbol{v}, \boldsymbol{v}) = 0$ for any $\boldsymbol{u}, \boldsymbol{v} \in \mathbf{H}_0^1(\Omega)$.

A substitution of $\xi = \lambda w$, $\varphi = \lambda \partial_t \phi$, $\boldsymbol{v} = \boldsymbol{u}$, $\boldsymbol{l} = \boldsymbol{B}$ and $q = p$ into (16)–(20) leads to

$$\begin{aligned}
&\frac{1}{2}\frac{\mathrm{d}}{\mathrm{d}t}\left(\|\boldsymbol{u}\|_{L^2}^2 + \mu\|\boldsymbol{B}\|_{L^2}^2 + \frac{\lambda}{2\varepsilon}\|\phi^2 - 1\|_{L^2}^2 + \lambda\varepsilon\|\nabla\phi\|_{L^2}^2 \right) \\
&\qquad + \lambda\varepsilon\|\nabla w\|_{L^2}^2 + \eta\|\nabla \boldsymbol{u}\|_{L^2}^2 + \sigma^{-1}\|\nabla \times \boldsymbol{B}\|_{L^2}^2 = 0.
\end{aligned}$$

Thus by removing the non-negative terms and defining the total free energy as

$$\Theta := \|\boldsymbol{u}\|_{L^2}^2 + \mu\|\boldsymbol{B}\|_{L^2}^2 + \frac{\lambda}{2\varepsilon}\|\phi^2 - 1\|_{L^2}^2 + \lambda\varepsilon\|\nabla\phi\|_{L^2}^2,$$

which is composed of the phase field free energy, and the kinematic and magnetic free energies, we get

$$\frac{\mathrm{d}\Theta}{\mathrm{d}t} \leq 0. \tag{22}$$

This gives the total free energy dissipation for the two-phase MHD model (6)–(10).

3. Numerical method and main results

In this section, we will present a second-order Crank–Nicolson finite element scheme for solving the system (6)–(10). The unique solvability, mass conservation, and unconditional energy stability of the scheme will be established as well.

3.1. Fully discrete numerical scheme and main results

Let $\mathfrak{T}_h$ be a quasi-uniform partition of Ω into tetrahedrons K_j in $\mathbb{R}^3$ (or triangles in $\mathbb{R}^2$), $j = 1, 2, \ldots, M$, with mesh size $h = \max_{1\le j\le M} \operatorname{diam}(K_j)$. To solve for the unknowns ϕ and w, the following finite element space is employed:

$$Y_h = \left\{ v_h \in H^1(\Omega) \mid v_h|_{K_j} \in P_r(K_j) \right\},$$

for any integer $r \ge 2$, where $P_r(K_j)$ stands for the space of polynomials with degree at most r in K_j. The Taylor–Hood elements are utilized to approximate $\boldsymbol{u}$ and p, and the corresponding finite element spaces are defined by

$$\begin{aligned}
\mathbf{X}_h &= \left\{ \boldsymbol{v}_h \in \mathbf{H}_0^1(\Omega) \mid \boldsymbol{v}_h|_{K_j} \in \mathbf{P}_r(K_j) \right\},\\
M_h &= \left\{ v_h \in L_0^2(\Omega) \mid v_h|_{K_j} \in P_{r-1}(K_j) \right\},
\end{aligned}$$

with $\mathbf{P}_r(K_j) = [P_r(K_j)]^d$. Moreover, the following finite element space is introduced for solving for $\boldsymbol{B}$:

$$\mathbf{S}_h = \left\{ \boldsymbol{v}_h \in \mathring{\mathbf{H}}^1(\Omega) \mid \boldsymbol{v}_h|_{K_j} \in \mathbf{P}_r(K_j) \right\}.$$

Let $\{t_n = n\tau\}_{n=0}^N$ be a uniform partition of the time interval $[0, T]$ with the time step size $\tau = T/N$. We denote by v^n the abbreviation for $v(\cdot, t^n)$, and then define

$$\begin{aligned}
\widetilde{v}^{n+\frac12} &:= \frac12(3v^n - v^{n-1}), \qquad & \overline{v}^{n+\frac12} &:= \frac12(v^{n+1} + v^n),\\
\breve{v}^{n+\frac12} &:= \frac14(3v^{n+1} + v^{n-1}), \qquad & \delta_\tau v^{n+\frac12} &:= \frac1\tau(v^{n+1} - v^n).
\end{aligned} \tag{23}$$

Based on finite element spatial approximation and a modified Crank–Nicolson temporal discretization, we propose a fully discrete scheme for solving the incompressible Cahn-Hilliard-MHD system (6)–(10): find $(\phi_h^{n+1}, w_h^{n+1}, \boldsymbol{u}_h^{n+1}, \boldsymbol{B}_h^{n+1}, p_h^{n+1}) \in (Y_h, Y_h, \mathbf{X}_h, \mathbf{S}_h, M_h)$, such that

$$\left(\delta_\tau \phi_h^{n+\frac12}, \xi_h\right) - \left(\widetilde{\phi}_h^{n+\frac12} \overline{\boldsymbol{u}}_h^{n+\frac12}, \nabla\xi_h\right) + \varepsilon\left(\nabla \overline{w}_h^{n+\frac12}, \nabla\xi_h\right) = 0, \tag{24}$$

$$\varepsilon^{-1}\left(\overline{\phi}_h^{n+\frac12} \frac{(\phi_h^{n+1})^2 + (\phi_h^n)^2}{2}, \varphi_h\right) - \varepsilon^{-1}\left(\widetilde{\phi}_h^{n+\frac12}, \varphi_h\right) + \varepsilon\left(\nabla \breve{\phi}_h^{n+\frac12}, \nabla\varphi_h\right) = \left(\overline{w}_h^{n+\frac12}, \varphi_h\right), \tag{25}$$

$$\begin{aligned}
&\left(\delta_\tau \boldsymbol{u}_h^{n+\frac12}, \boldsymbol{v}_h\right) + b\left(\widetilde{\boldsymbol{u}}_h^{n+\frac12}, \overline{\boldsymbol{u}}_h^{n+\frac12}, \boldsymbol{v}_h\right) + \eta\left(\nabla \overline{\boldsymbol{u}}_h^{n+\frac12}, \nabla \boldsymbol{v}_h\right) - \left(\overline{p}_h^{n+\frac12}, \nabla\cdot\boldsymbol{v}_h\right)\\
&\qquad + \lambda\left(\widetilde{\phi}_h^{n+\frac12} \nabla \overline{w}_h^{n+\frac12}, \boldsymbol{v}_h\right) = \mu\left((\nabla\times\overline{\boldsymbol{B}}_h^{n+\frac12}) \times \widetilde{\boldsymbol{B}}_h^{n+\frac12}, \boldsymbol{v}_h\right),
\end{aligned} \tag{26}$$

$$\begin{aligned}
&\mu\left(\delta_\tau \boldsymbol{B}_h^{n+\frac12}, \boldsymbol{l}_h\right) + \sigma^{-1}\left(\nabla\times\overline{\boldsymbol{B}}_h^{n+\frac12}, \nabla\times\boldsymbol{l}_h\right) + \sigma^{-1}\left(\nabla\cdot\overline{\boldsymbol{B}}_h^{n+\frac12}, \nabla\cdot\boldsymbol{l}_h\right)\\
&\qquad - \mu\left(\overline{\boldsymbol{u}}_h^{n+\frac12} \times \widetilde{\boldsymbol{B}}_h^{n+\frac12}, \nabla\times\boldsymbol{l}_h\right) = 0,
\end{aligned} \tag{27}$$

$$\left(\nabla\cdot\boldsymbol{u}_h^{n+1}, q_h\right) = 0 \tag{28}$$

for any $(\xi_h, \varphi_h, \boldsymbol{v}_h, \boldsymbol{l}_h, q_h) \in (Y_h, Y_h, \mathbf{X}_h, \mathbf{S}_h, M_h)$, and $n = 1, 2, \ldots, N-1$.

For the error estimates, we shall assume the following regularities of solutions:

$$\begin{aligned}
&\phi \in W^{1,\infty}(0,T; H^{r+1}(\Omega)) \cap H^2(0,T; H^3(\Omega)) \cap C^3(0,T; L^2(\Omega)),\\
&\phi^2 \in H^2(0,T; H^1(\Omega)),\\
&w \in L^\infty(0,T; H^{r+1}(\Omega)),\\
&\boldsymbol{u} \in \mathbf{W}^{1,\infty}(0,T; \mathbf{H}^{r+1}(\Omega)) \cap \mathbf{H}^2(0,T; \mathbf{H}^3(\Omega)) \cap \mathbf{C}^3(0,T; \mathbf{L}^2(\Omega)),\\
&\boldsymbol{B} \in \mathbf{W}^{1,\infty}(0,T; \mathbf{H}^{r+1}(\Omega)) \cap \mathbf{H}^2(0,T; \mathbf{H}^3(\Omega)) \cap \mathbf{C}^3(0,T; \mathbf{L}^2(\Omega)),\\
&p \in L^\infty(0,T; H^r(\Omega)) \cap L_0^2(\Omega),
\end{aligned}$$

where $r \ge 2$ is the spatial approximation order. Then, we have the following results of the numerical scheme (24)–(28).

Theorem 3.1. *Assume that the solution $(\phi, w, \boldsymbol{u}, \boldsymbol{B}, p)$ of the CH-MHD system (6)–(10) is sufficiently smooth. Then, there exists a positive constant τ_0 such that when $\tau < \tau_0$, the following error estimates could be established for the numerical* *scheme (24)–(28):*

$$\max_{1\le n\le N-1}\Big(\|\nabla(\phi^{n+1}-\phi_h^{n+1})\|_{L^2}+\|\boldsymbol{u}^{n+1}-\boldsymbol{u}_h^{n+1}\|_{L^2}+\|\boldsymbol{B}^{n+1}-\boldsymbol{B}_h^{n+1}\|_{L^2}\Big)\le C_0(h^r+\tau^2), \tag{29}$$

$$\tau\sum_{n=1}^{N-1}\Big(\|\nabla(\overline{w}^{n+\frac12}-\overline{w}_h^{n+\frac12})\|_{L^2}^2+\|\nabla(\overline{\boldsymbol{u}}^{n+\frac12}-\overline{\boldsymbol{u}}_h^{n+\frac12})\|_{L^2}^2+\|\nabla\cdot(\overline{\boldsymbol{B}}^{n+\frac12}-\overline{\boldsymbol{B}}_h^{n+\frac12})\|_{L^2}^2 + \|\nabla\times(\overline{\boldsymbol{B}}^{n+\frac12}-\overline{\boldsymbol{B}}_h^{n+\frac12})\|_{L^2}^2\Big)^{\frac12}\le C_0(h^r+\tau^2), \tag{30}$$

where C_0 is a positive constant independent of h, τ, and n.

The proof of Theorem 3.1 will be given in Section 4.

Remark 3.1. A stabilized term $\sigma^{-1}\big(\nabla\cdot\overline{\boldsymbol{B}}_h^{n+\frac12},\nabla\cdot\boldsymbol{l}_h\big)$ has been added to ensure the coercivity of the magnetic equation, which will facilitate the analysis of unique solvability of Eq. (27).

Remark 3.2. In this paper, the Crank–Nicolson method enables us to obtain unconditional energy stability for the numerical scheme. It is straightforward to extend the Crank–Nicolson scheme to the case of nonuniform meshes and the corresponding theoretical analyses are similar. Note that a modified Crank–Nicolson approximation has been applied to the chemical potential associated with the double-well energy potential. The resulting nonlinear system could be solved effectively by using the Newton's iteration method, due to the fact that the nonlinear term in (25) is convex. To avoid the nonlinearity of the numerical scheme, an alternative approach based on the invariant energy quadratization (IEQ) method can be used, which results in a linear discrete scheme and can maintain a discrete IEQ modified energy dissipation law (cf. [48,49] and the references therein).

Remark 3.3. For the sake of brevity, we assume that the numerical solutions at the first time step are given and satisfy the estimates (29)–(30). One approach to constructing numerical schemes at the first time step is to use methods such as the Crank–Nicolson method or the backward Euler method with a very small time size. Then the resulting schemes satisfy the convergence in (29)–(30).

Remark 3.4. A temporal discretization $\nabla\breve{\phi}_h^{n+\frac12}=\frac34\nabla\phi_h^{n+1}+\frac14\nabla\phi_h^{n-1}$, i.e., the modified Crank–Nicolson method, is used in (25) to ensure the bound of $\|\phi_h^n\|_{L^\infty}$; see Lemma 4.4.

Remark 3.5. In this work, we focus on the error estimates of $\boldsymbol{u},\boldsymbol{B},\phi,w$. The error estimate of p can be obtained by using the discrete inf–sup condition. For the sake of brevity, we omit the proof and refer readers to [50] for more details. Theoretical results in Theorem 3.1 show that the spatial convergence orders for ϕ, w, and $\boldsymbol{u}$ are optimal in H^1 semi-norm.

In this paper, we denote by C a generic positive constant which could vary at different places and by ζ a generic small positive constant, which are independent of n, h, τ, and C_0.

3.2. Discrete mass conservation and unconditional energy stability

Theorem 3.2. *The fully discrete FEM system (24)–(28) admits a unique solution, for any $\tau>0$ and $h>0$, and, in addition, the following discrete mass conservation is valid:*

$$\int_\Omega\phi_h^{n+1}d\boldsymbol{x}=\int_\Omega\phi_h^0 d\boldsymbol{x}, \tag{31}$$

for $n=1,2,\ldots,N-1$. Furthermore, the numerical solution $(\phi_h^n, w_h^{n-\frac12},\boldsymbol{u}_h^n,\boldsymbol{B}_h^n,p_h^n)$ to the fully discrete scheme (24)–(28) satisfies the following discrete energy estimate:

$$\Theta_h^{n+1}\le\Theta_h^n, \tag{32}$$

for any $n=1,2,\ldots,N-1$, where

$$\Theta_h^n:=\frac{\lambda}{2\varepsilon}\Big(\|(\phi_h^n)^2-1\|_{L^2}^2+\|\phi_h^n-\phi_h^{n-1}\|_{L^2}^2\Big)+\lambda\varepsilon\Big(\|\nabla\phi_h^n\|_{L^2}^2+\frac14\|\nabla\phi_h^n-\nabla\phi_h^{n-1}\|_{L^2}^2\Big) + \|\boldsymbol{u}_h^n\|_{L^2}^2+\mu\|\boldsymbol{B}_h^n\|_{L^2}^2, \tag{33}$$

for any time step size $\tau>0$ and any space step size $h>0$.

Proof. Following similar arguments to those as given in [1, Theorem 4.5], we can get the unconditional unique solvability of solutions of system (24)–(28). We will suppress that argument for the sake of brevity.

To obtain the discrete mass conservation, we take $\xi_h = 1$ in (24) and get

$$(\delta_\tau \phi_h^{n+\frac{1}{2}}, 1) = 0,$$

which yields the discrete mass conservation equality (31).

Next we proceed with the proof of discrete energy stability. Taking $\xi_h = \lambda \overline{w}_h^{n+\frac{1}{2}}, \varphi_h = \lambda \delta_\tau \phi_h^{n+\frac{1}{2}}, \boldsymbol{v}_h = \overline{\boldsymbol{u}}_h^{n+\frac{1}{2}}, \boldsymbol{l}_h = \overline{\boldsymbol{B}}_h^{n+\frac{1}{2}}, q_h = \overline{p}_h^{n+\frac{1}{2}}$ in (24)–(28), respectively, and summing up the resulting equations lead to

$$\begin{aligned}
&\lambda\varepsilon^{-1}\Big(\overline{\phi}_h^{n+\frac{1}{2}}\frac{(\phi_h^{n+1})^2+(\phi_h^n)^2}{2} - \widetilde{\phi}_h^{n+\frac{1}{2}}, \delta_\tau\phi_h^{n+\frac{1}{2}}\Big) + \lambda\varepsilon\big(\nabla\breve{\phi}_h^{n+\frac{1}{2}}, \nabla\delta_\tau\phi_h^{n+\frac{1}{2}}\big) \\
&\quad + \lambda\varepsilon\|\nabla\overline{w}_h^{n+\frac{1}{2}}\|_{L^2}^2 + \big(\delta_\tau\boldsymbol{u}_h^{n+\frac{1}{2}}, \overline{\boldsymbol{u}}_h^{n+\frac{1}{2}}\big) + \mu\big(\delta_\tau\boldsymbol{B}_h^{n+\frac{1}{2}}, \overline{\boldsymbol{B}}_h^{n+\frac{1}{2}}\big) \\
&\quad + \eta\|\nabla\overline{\boldsymbol{u}}_h^{n+\frac{1}{2}}\|_{L^2}^2 + \sigma^{-1}\|\nabla\times\overline{\boldsymbol{B}}_h^{n+\frac{1}{2}}\|_{L^2}^2 + \sigma^{-1}\|\nabla\cdot\overline{\boldsymbol{B}}_h^{n+\frac{1}{2}}\|_{L^2}^2 = 0.
\end{aligned} \tag{34}$$

With the help of the following identities

$$\left(\frac{3}{4}a + \frac{1}{4}c\right)(a-b) = \frac{1}{2}(a^2-b^2) + \frac{1}{8}[(a-b)^2 - (b-c)^2 + (a-2b+c)^2],$$

$$\begin{aligned}
\left(\frac{a+b}{2}\frac{a^2+b^2}{2} - \frac{3b-c}{2}\right)(a-b) = \frac{1}{4}[&(a^2-1)^2 - (b^2-1)^2 \\
&+ (a-b)^2 - (b-c)^2 + (a-2b+c)^2],
\end{aligned}$$

(34) becomes

$$\begin{aligned}
&\frac{\lambda\varepsilon^{-1}}{4\tau}(\|(\phi_h^{n+1})^2-1\|_{L^2}^2 - \|(\phi_h^n)^2-1\|_{L^2}^2 + \|\phi_h^{n+1}-\phi_h^n\|_{L^2}^2 - \|\phi_h^n-\phi_h^{n-1}\|_{L^2}^2 \\
&+ \|\phi_h^{n+1}-2\phi_h^n+\phi_h^{n-1}\|_{L^2}^2) + \frac{\lambda\varepsilon}{8\tau}(4\|\nabla\phi_h^{n+1}\|_{L^2}^2 - 4\|\nabla\phi_h^n\|_{L^2}^2 \\
&+ \|\nabla(\phi_h^{n+1}-\phi_h^n)\|_{L^2}^2 - \|\nabla(\phi_h^n-\phi_h^{n-1})\|_{L^2}^2 + \|\nabla(\phi_h^{n+1}-2\phi_h^n+\phi_h^{n-1})\|_{L^2}^2) \\
&+ \frac{1}{2\tau}(\|\boldsymbol{u}_h^{n+1}\|_{L^2} - \|\boldsymbol{u}_h^n\|_{L^2}^2 + \mu\|\boldsymbol{B}_h^{n+1}\|_{L^2}^2 - \mu\|\boldsymbol{B}_h^n\|_{L^2}^2) \\
&+ \lambda\varepsilon\|\nabla\overline{w}_h^{n+\frac{1}{2}}\|_{L^2}^2 + \eta\|\nabla\overline{\boldsymbol{u}}_h^{n+\frac{1}{2}}\|_{L^2}^2 + \sigma^{-1}\|\nabla\cdot\overline{\boldsymbol{B}}_h^{n+\frac{1}{2}}\|_{L^2}^2 + \sigma^{-1}\|\nabla\times\overline{\boldsymbol{B}}_h^{n+\frac{1}{2}}\|_{L^2}^2 = 0.
\end{aligned} \tag{35}$$

The discrete energy stability (32) follows immediately for $n = 1, 2, \ldots, N-1$.

Meanwhile, (35) also leads to the boundness of the numerical solution that

$$\max_{2\le n\le N}\Big(\|(\phi_h^n)^2\|_{L^2} + \|\nabla\phi_h^n\|_{L^2} + \|\boldsymbol{u}_h^n\|_{L^2} + \|\boldsymbol{B}_h^n\|_{L^2}\Big) \le C, \tag{36}$$

$$\tau\sum_{n=1}^{N-1}\Big(\|\nabla\overline{w}_h^{n+\frac{1}{2}}\|_{L^2}^2 + \|\nabla\overline{\boldsymbol{u}}_h^{n+\frac{1}{2}}\|_{L^2}^2 + \|\nabla\cdot\overline{\boldsymbol{B}}_h^{n+\frac{1}{2}}\|_{L^2}^2 + \|\nabla\times\overline{\boldsymbol{B}}_h^{n+\frac{1}{2}}\|_{L^2}^2\Big) \le C, \tag{37}$$

which will be used in the error estimates in the next section. □

4. Error estimates

In this section we carry out error estimates of the numerical scheme (24)–(28), as given by Theorem 3.1.

4.1. Some preliminary results

First of all, we introduce several projections and the corresponding consistency estimates. The Ritz projection $Q_h : H^1(\Omega) \to Y_h$ is defined by

$$(\nabla(v - Q_h v), \nabla v_h) = 0, \quad v \in H^1(\Omega), \quad \forall v_h \in Y_h, \tag{38}$$

with $\int_\Omega (v - Q_h v)\, d\mathbf{x} = 0$. The Stokes projection $(\boldsymbol{R}_h\boldsymbol{u}, R_h p)$ of $(\boldsymbol{u}, p) \in \mathbf{H}_0^1(\Omega)\times L_0^2(\Omega)$ is defined by

$$\eta(\nabla(\boldsymbol{u} - \boldsymbol{R}_h\boldsymbol{u}), \nabla\boldsymbol{v}_h) - (p - R_h p, \nabla\cdot\boldsymbol{v}_h) = 0, \qquad \forall\boldsymbol{v}_h \in \mathbf{X}_h, \tag{39}$$

$$(\nabla\cdot(\boldsymbol{u} - \boldsymbol{R}_h\boldsymbol{u}), q_h) = 0, \qquad \forall q_h \in M_h. \tag{40}$$

Furthermore, $\Pi_h : \mathring{\mathbf{H}}^1(\Omega) \to \mathbf{S}_h$ denotes the Maxwell projection satisfying

$$\big(\nabla\times(\boldsymbol{B} - \Pi_h\boldsymbol{B}), \nabla\times\boldsymbol{l}_h\big) + \big(\nabla\cdot(\boldsymbol{B} - \Pi_h\boldsymbol{B}), \nabla\cdot\boldsymbol{l}_h\big) = 0, \quad \boldsymbol{B}\in\mathring{\mathbf{H}}^1(\Omega), \quad \forall\boldsymbol{l}_h\in\mathbf{S}_h. \tag{41}$$

In the following, we recall several existing results, which will be used frequently in the proof of Theorem 3.1.

Lemma 4.1 (*[51–53]*). *The following inequalities hold for the Ritz projection, Stokes projection, and Maxwell projection:*

$$\|v - Q_h v\|_{L^2} + h\|v - Q_h v\|_{H^1} \le Ch^{\ell+1}\|v\|_{H^{\ell+1}}, \tag{42}$$

for $0 \le \ell \le r$,

$$\|\boldsymbol{R}_h\boldsymbol{u}\|_{W^{1,4}} + \|\boldsymbol{R}_h\boldsymbol{u}\|_{L^\infty} \le C(\|\boldsymbol{u}\|_{H^2} + \|p\|_{H^1}), \tag{43}$$

$$\|\boldsymbol{u} - \boldsymbol{R}_h\boldsymbol{u}\|_{L^2} + h\|\boldsymbol{u} - \boldsymbol{R}_h\boldsymbol{u}\|_{H^1} \le Ch^{\ell+1}(\|\boldsymbol{u}\|_{H^{\ell+1}} + \|p\|_{H^\ell}), \tag{44}$$

$$\|p - R_h p\|_{L^2} \le Ch^{\ell}(\|\boldsymbol{u}\|_{H^{\ell+1}} + \|p\|_{H^\ell}), \tag{45}$$

for $0 \le \ell \le r$, *and*

$$\|\boldsymbol{B} - \Pi_h\boldsymbol{B}\|_{L^2} + h\|\boldsymbol{B} - \Pi_h\boldsymbol{B}\|_{H^1} \le Ch^{r+1}\|\boldsymbol{B}\|_{H^{r+1}}. \tag{46}$$

for $0 \le \ell \le r$, *where* C *is a positive constant independent of* h.

Lemma 4.2 (*[51]*). *For any* v_h *in the finite spaces* Y_h, M_h, $\boldsymbol{X}_h$, *or* $\boldsymbol{S}_h$, *it holds that*

$$\|v_h\|_{W^{m,s}} \le Ch^{n-m+\frac{d}{s}-\frac{d}{q}}\|v_h\|_{W^{n,q}}, \tag{47}$$

for $0 \le n \le m \le 1$, $1 \le q \le s \le \infty$, *where* d *is the dimension of the space, and* C *is a positive constant independent of* h.

Let $\mathring{Y}_h := Y_h \cap L_0^2(\Omega)$. We define a linear operator $T_h : \mathring{Y}_h \to \mathring{Y}_h$ such that for given $v_h \in \mathring{Y}_h$,

$$(\nabla T_h v_h, \nabla \xi_h) = (v_h, \xi_h), \quad \forall \xi_h \in \mathring{Y}_h. \tag{48}$$

Then for $v_h, \xi_h \in \mathring{Y}_h$, the discrete H^{-1} inner product is introduced as

$$(v_h, \xi_h)_{-1,h} := (T_h v_h, \xi_h). \tag{49}$$

It is known [36, Lemma 2.6] that $(\cdot,\cdot)_{-1,h}$ defines an inner product on $\mathring{Y}_h$, and the induced negative norm is given by

$$\|v_h\|_{-1,h} := \sqrt{(v_h, v_h)_{-1,h}}. \tag{50}$$

For the above negative norm, we have the following result.

Lemma 4.3 (*[36, Lemma 2.6]*). *For all* $\chi \in Y_h$ *and all* $v_h \in \mathring{Y}_h$, *it holds that*

$$(v_h, \chi) \le C\|v_h\|_{-1,h}\|\nabla\chi\|_{L^2}, \tag{51}$$

where C *is a positive constant independent of* h.

In the error estimates of the numerical scheme (24)–(28), the following lemma will be frequently used.

Lemma 4.4. *The numerical solution* ϕ_h^n *to the system* (24)–(28) *satisfies*

$$\|\phi_h^n\|_{L^\infty} + \|\nabla\phi_h^n\|_{L^3} \le C(T+1), \tag{52}$$

where C *is a positive constant independent of* h, τ, *and* T *(the final time).*

Proof. We refer to Proposition 2.8, Lemma 2.10, and Lemma 2.13 in [37] for the proof of estimate (52). The details are basically the same. □

4.2. Error equations

With the projections defined in the previous subsection, we rewrite Eqs. (16)–(20) into the following form:

$$\left(\delta_\tau Q_h\phi^{n+\frac12}, \xi_h\right) - \left(\widetilde{\phi}^{n+\frac12}\overline{\boldsymbol{u}}^{n+\frac12}, \nabla\xi_h\right) + \varepsilon\left(\nabla Q_h\overline{w}^{n+\frac12}, \nabla\xi_h\right) = T_\phi(\xi_h), \tag{53}$$

$$\begin{aligned}\varepsilon^{-1}\Big(\overline{\phi}^{n+\frac12}\frac{(\phi^{n+1})^2+(\phi^n)^2}{2}, \varphi_h\Big) - \varepsilon^{-1}\left(Q_h\widetilde{\phi}^{n+\frac12}, \varphi_h\right) + \varepsilon\left(\nabla Q_h\breve{\phi}^{n+\frac12}, \nabla\varphi_h\right)&\\ = \left(Q_h\overline{w}^{n+\frac12}, \varphi_h\right) + T_w(\varphi_h),&\end{aligned} \tag{54}$$

$$\begin{aligned}\left(\delta_\tau\boldsymbol{R}_h\boldsymbol{u}^{n+\frac12}, \boldsymbol{v}_h\right) + b\left(\widetilde{\boldsymbol{u}}^{n+\frac12}, \overline{\boldsymbol{u}}^{n+\frac12}, \boldsymbol{v}_h\right) + \eta\left(\nabla\boldsymbol{R}_h\overline{\boldsymbol{u}}^{n+\frac12}, \nabla\boldsymbol{v}_h\right) - \left(R_h\overline{p}^{n+\frac12}, \nabla\cdot\boldsymbol{v}_h\right)&\\ + \lambda\left(\widetilde{\phi}^{n+\frac12}\nabla\overline{w}^{n+\frac12}, \boldsymbol{v}_h\right) = \mu\left((\nabla\times\overline{\boldsymbol{B}}^{n+\frac12})\times\widetilde{\boldsymbol{B}}^{n+\frac12}, \boldsymbol{v}_h\right) + T_{\boldsymbol{u}}(\boldsymbol{v}_h),&\end{aligned} \tag{55}$$

$$\mu\big(\delta_\tau \Pi_h \boldsymbol{B}^{n+\frac{1}{2}}, \boldsymbol{l}_h\big) + \sigma^{-1}\big(\nabla\times \Pi_h \overline{\boldsymbol{B}}^{n+\frac{1}{2}}, \nabla\times \boldsymbol{l}_h\big) + \sigma^{-1}\big(\nabla\cdot \Pi_h \overline{\boldsymbol{B}}^{n+\frac{1}{2}}, \nabla\cdot \boldsymbol{l}_h\big)$$
$$- \mu\big(\overline{\boldsymbol{u}}^{n+\frac{1}{2}} \times \widetilde{\boldsymbol{B}}^{n+\frac{1}{2}}, \nabla\times \boldsymbol{l}_h\big) = T_{\boldsymbol{B}}(\boldsymbol{l}_h), \tag{56}$$
$$\big(\nabla\cdot \boldsymbol{R}_h \boldsymbol{u}^{n+1}, q_h\big) = 0, \tag{57}$$

for any $(\xi_h, \varphi_h, \boldsymbol{v}_h, \boldsymbol{l}_h, q_h) \in (Y_h, Y_h, \mathbf{X}_h, \mathbf{S}_h, M_h)$, and $1 \le n \le N$. Here, the truncation error terms T_ϕ, T_w, $T_{\boldsymbol{u}}$, $T_{\boldsymbol{B}}$, T_p are given by

$$\begin{aligned}
T_\phi(\xi_h) =& \big(\delta_\tau Q_h \phi^{n+\frac{1}{2}} - \partial_t \phi^{n+\frac{1}{2}}, \xi_h\big) + \varepsilon\big(\nabla(\overline{w}^{n+\frac{1}{2}} - w^{n+\frac{1}{2}}), \nabla\xi_h\big) \\
&- \big(\widetilde{\phi}^{n+\frac{1}{2}} \overline{\boldsymbol{u}}^{n+\frac{1}{2}} - \phi^{n+\frac{1}{2}} \boldsymbol{u}^{n+\frac{1}{2}}, \nabla\xi_h\big), \\
T_w(\varphi_h) =& \varepsilon^{-1}\big(\overline{\phi}^{n+\frac{1}{2}} \frac{(\phi^{n+1})^2 + (\phi^n)^2}{2} - (\phi^{n+\frac{1}{2}})^3, \varphi_h\big) - \varepsilon^{-1}\big(Q_h \widetilde{\phi}^{n+\frac{1}{2}} - \phi^{n+\frac{1}{2}}, \varphi_h\big) \\
&+ \varepsilon\big(\nabla(\breve{\phi}^{n+\frac{1}{2}} - \phi^{n+\frac{1}{2}}), \nabla\varphi_h\big) + \big(w^{n+\frac{1}{2}} - Q_h \overline{w}^{n+\frac{1}{2}}, \varphi_h\big), \\
T_{\boldsymbol{u}}(\boldsymbol{v}_h) =& \big(\delta_\tau \boldsymbol{R}_h \boldsymbol{u}^{n+\frac{1}{2}} - \partial_t \boldsymbol{u}^{n+\frac{1}{2}}, \boldsymbol{v}_h\big) + b\big(\widetilde{\boldsymbol{u}}^{n+\frac{1}{2}}, \overline{\boldsymbol{u}}^{n+\frac{1}{2}}, \boldsymbol{v}_h\big) - b\big(\boldsymbol{u}^{n+\frac{1}{2}}, \boldsymbol{u}^{n+\frac{1}{2}}, \boldsymbol{v}_h\big) \\
&+ \eta\big(\nabla(\overline{\boldsymbol{u}}^{n+\frac{1}{2}} - \boldsymbol{u}^{n+\frac{1}{2}}), \nabla\boldsymbol{v}_h\big) - \big(\overline{p}^{n+\frac{1}{2}} - p^{n+\frac{1}{2}}, \nabla\cdot v_h\big) \\
&+ \lambda\big(\widetilde{\phi}^{n+\frac{1}{2}} \nabla\overline{w}^{n+\frac{1}{2}} - \phi^{n+\frac{1}{2}} \nabla w^{n+\frac{1}{2}}, \boldsymbol{v}_h\big) \\
&- \mu\big((\nabla\times \overline{\boldsymbol{B}}^{n+\frac{1}{2}}) \times \widetilde{\boldsymbol{B}}^{n+\frac{1}{2}} - (\nabla\times \boldsymbol{B}^{n+\frac{1}{2}}) \times \boldsymbol{B}^{n+\frac{1}{2}}, \boldsymbol{v}_h\big), \\
T_{\boldsymbol{B}}(\boldsymbol{l}_h) =& \mu\big(\delta_\tau \Pi_h \boldsymbol{B}^{n+\frac{1}{2}} - \partial_t \boldsymbol{B}^{n+\frac{1}{2}}, \boldsymbol{l}_h\big) - \mu\big(\overline{\boldsymbol{u}}^{n+\frac{1}{2}} \times \widetilde{\boldsymbol{B}}^{n+\frac{1}{2}} - \boldsymbol{u}^{n+\frac{1}{2}} \times \boldsymbol{B}^{n+\frac{1}{2}}, \nabla\times \boldsymbol{l}_h\big) \\
&+ \sigma^{-1}\big(\nabla\times (\overline{\boldsymbol{B}}^{n+\frac{1}{2}} - \boldsymbol{B}^{n+\frac{1}{2}}), \nabla\times \boldsymbol{l}_h\big) + \sigma^{-1}\big(\nabla\cdot (\overline{\boldsymbol{B}}^{n+\frac{1}{2}} - \boldsymbol{B}^{n+\frac{1}{2}}), \nabla\cdot \boldsymbol{l}_h\big).
\end{aligned}$$

Now, we analyze the errors between the numerical solutions and the projection functions and thus define

$$\begin{aligned}
&e_\phi^n := Q_h \phi^n - \phi_h^n, \quad e_w^n := Q_h w^n - w_h^n, \\
&e_{\boldsymbol{u}}^n := \boldsymbol{R}_h \boldsymbol{u}^n - \boldsymbol{u}_h^n, \quad e_{\boldsymbol{B}}^n := \Pi_h \boldsymbol{B}^n - \boldsymbol{B}_h^n, \quad e_p^n := R_h p^n - p_h^n.
\end{aligned}$$

Subtracting (24)–(28) from (53)–(57) yields a system of error evolutionary equations:

$$\big(\delta_\tau e_\phi^{n+\frac{1}{2}}, \xi_h\big) - \big(\widetilde{\phi}^{n+\frac{1}{2}} \overline{\boldsymbol{u}}^{n+\frac{1}{2}} - \widetilde{\phi}_h^{n+\frac{1}{2}} \overline{\boldsymbol{u}}_h^{n+\frac{1}{2}}, \nabla\xi_h\big) + \varepsilon\big(\nabla\overline{e}_w^{n+\frac{1}{2}}, \nabla\xi_h\big) = T_\phi(\xi_h), \tag{58}$$
$$\varepsilon^{-1}\big(\overline{\phi}^{n+\frac{1}{2}} \frac{(\phi^{n+1})^2 + (\phi^n)^2}{2} - \overline{\phi}_h^{n+\frac{1}{2}} \frac{(\phi_h^{n+1})^2 + (\phi_h^n)^2}{2}, \varphi_h\big) - \varepsilon^{-1}\big(\widetilde{e}_\phi^{n+\frac{1}{2}}, \varphi_h\big)$$
$$+ \varepsilon\big(\nabla\breve{e}_\phi^{n+\frac{1}{2}}, \nabla\varphi_h\big) = \big(\overline{e}_w^{n+\frac{1}{2}}, \varphi_h\big) + T_w(\varphi_h), \tag{59}$$
$$\big(\delta_\tau e_{\boldsymbol{u}}^{n+\frac{1}{2}}, \boldsymbol{v}_h\big) + b\big(\widetilde{\boldsymbol{u}}^{n+\frac{1}{2}}, \overline{\boldsymbol{u}}^{n+\frac{1}{2}}, \boldsymbol{v}_h\big) - b\big(\widetilde{\boldsymbol{u}}_h^{n+\frac{1}{2}}, \overline{\boldsymbol{u}}_h^{n+\frac{1}{2}}, \boldsymbol{v}_h\big) - \big(\overline{e}_p^{n+\frac{1}{2}}, \nabla\cdot \boldsymbol{v}_h\big)$$
$$+ \eta\big(\nabla\overline{e}_{\boldsymbol{u}}^{n+\frac{1}{2}}, \nabla\boldsymbol{v}_h\big) + \lambda\big(\widetilde{\phi}^{n+\frac{1}{2}} \nabla\overline{w}^{n+\frac{1}{2}} - \widetilde{\phi}_h^{n+\frac{1}{2}} \nabla\overline{w}_h^{n+\frac{1}{2}}, \boldsymbol{v}_h\big)$$
$$= \mu\big((\nabla\times \overline{\boldsymbol{B}}^{n+\frac{1}{2}}) \times \widetilde{\boldsymbol{B}}^{n+\frac{1}{2}} - (\nabla\times \overline{\boldsymbol{B}}_h^{n+\frac{1}{2}}) \times \widetilde{\boldsymbol{B}}_h^{n+\frac{1}{2}}, \boldsymbol{v}_h\big) + T_{\boldsymbol{u}}(\boldsymbol{v}_h), \tag{60}$$
$$\mu\big(\delta_\tau e_{\boldsymbol{B}}^{n+\frac{1}{2}}, \boldsymbol{l}_h\big) + \sigma^{-1}\big(\nabla\times \overline{e}_{\boldsymbol{B}}^{n+\frac{1}{2}}, \nabla\times \boldsymbol{l}_h\big) + \sigma^{-1}\big(\nabla\cdot \overline{e}_{\boldsymbol{B}}^{n+\frac{1}{2}}, \nabla\cdot \boldsymbol{l}_h\big)$$
$$- \mu\big(\overline{\boldsymbol{u}}^{n+\frac{1}{2}} \times \widetilde{\boldsymbol{B}}^{n+\frac{1}{2}} - \overline{\boldsymbol{u}}_h^{n+\frac{1}{2}} \times \widetilde{\boldsymbol{B}}_h^{n+\frac{1}{2}}, \nabla\times \boldsymbol{l}_h\big) = T_{\boldsymbol{B}}(\boldsymbol{l}_h), \tag{61}$$
$$\big(\nabla\cdot e_{\boldsymbol{u}}^{n+1}, q_h\big) = 0, \tag{62}$$

for any $(\xi_h, \varphi_h, \boldsymbol{v}_h, \boldsymbol{l}_h, q_h) \in (Y_h, Y_h, \mathbf{X}_h, \mathbf{S}_h, M_h)$, and $n = 1, 2, \ldots, N-1$.

In the following subsection, we will analyze the above error equations and present the proof of Theorem 3.1.

4.3. Proof of Theorem 3.1

Proof. Step 1: Substituting $\xi_h = \overline{e}_w^{n+\frac{1}{2}}$ in (58) and $\varphi_h = \delta_\tau e_\phi^{n+\frac{1}{2}}$ in (59) gives

$$\begin{aligned}
&\frac{\varepsilon}{2\tau}(\|\nabla e_\phi^{n+1}\|_{L^2}^2 - \|\nabla e_\phi^n\|_{L^2}^2) + \varepsilon\|\nabla\overline{e}_w^{n+\frac{1}{2}}\|_{L^2}^2 + \frac{\varepsilon}{8\tau}(\|\nabla(e_\phi^{n+1} - e_\phi^n)\|_{L^2}^2 - \|\nabla(e_\phi^n - e_\phi^{n-1})\|_{L^2}^2 \\
&+ \|\nabla(e_\phi^{n+1} - 2e_\phi^n + e_\phi^{n-1})\|_{L^2}^2) \\
&= -\varepsilon^{-1}\big(\overline{\phi}^{n+\frac{1}{2}} \frac{(\phi^{n+1})^2 + (\phi^n)^2}{2} - \overline{\phi}_h^{n+\frac{1}{2}} \frac{(\phi_h^{n+1})^2 + (\phi_h^n)^2}{2}, \delta_\tau e_\phi^{n+\frac{1}{2}}\big) + \varepsilon^{-1}\big(\widetilde{e}_\phi^{n+\frac{1}{2}}, \delta_\tau e_\phi^{n+\frac{1}{2}}\big)
\end{aligned}$$

$$
\begin{aligned}
&+\big(\widetilde{\phi}^{n+\frac12}\overline{\boldsymbol{u}}^{n+\frac12}-\widetilde{\phi}_h^{n+\frac12}\overline{\boldsymbol{u}}_h^{n+\frac12},\nabla\overline{e}_w^{n+\frac12}\big)+T_\phi(\overline{e}_w^{n+\frac12})+T_w(\delta_\tau e_\phi^{n+\frac12})\\
:=&\sum_{i=1}^{5}I_{1,i}.
\end{aligned}\tag{63}
$$

Now, we estimate $I_{1,i}$, $i=1,2,\ldots,5$, respectively. By applying Lemma 4.4, it can be proved that [36, Lemma 3.6]

$$
\begin{aligned}
I_{1,1}=&-\frac{\varepsilon^{-1}}{4}\Big[\big((\phi^{n+1})^3-(\phi_h^{n+1})^3,\delta_\tau e_\phi^{n+\frac12}\big)+\big((\phi^{n+1})^2\phi^n-(\phi_h^{n+1})^2\phi_h^n,\delta_\tau e_\phi^{n+\frac12}\big)\\
&+\big(\phi^{n+1}(\phi^n)^2-\phi_h^{n+1}(\phi_h^n)^2,\delta_\tau e_\phi^{n+\frac12}\big)+\big((\phi^n)^3-(\phi_h^n)^3,\delta_\tau e_\phi^{n+\frac12}\big)\Big]\\
\le& C\|\nabla(\phi^{n+1}-\phi_h^{n+1})\|_{L^2}^2+C\|\nabla(\phi^n-\phi_h^n)\|_{L^2}^2+\zeta\|\delta_\tau e_\phi^{n+\frac12}\|_{-1,h}^2\\
\le& C(h^{2r}+\|\nabla e_\phi^{n+1}\|_{L^2}^2+\|\nabla e_\phi^n\|_{L^2}^2)+\zeta\|\delta_\tau e_\phi^{n+\frac12}\|_{-1,h}^2,
\end{aligned}
$$

where we have used (42) in the last inequality and ζ is a generic small positive constant independent of n, h, τ, and C_0. By using (51), the analysis of $I_{1,2}$ is straightforward:

$$
I_{1,2}=\varepsilon^{-1}\big(\widetilde{e}_\phi^{n+\frac12},\delta_\tau e_\phi^{n+\frac12}\big)\le C\|\nabla\widetilde{e}_\phi^{n+\frac12}\|_{L^2}^2+\zeta\|\delta_\tau e_\phi^{n+\frac12}\|_{-1,h}^2.
$$

To estimate $I_{1,3}$, we define

$$
\overline{\overline{e}_w^{n+\frac12}}:=|\Omega|^{-1}\big(\overline{e}_w^{n+\frac12},1\big).
$$

Since

$$
\|\overline{e}_w^{n+\frac12}-\overline{\overline{e}_w^{n+\frac12}}\|_{L^2}\le C\|\nabla(\overline{e}_w^{n+\frac12}-\overline{\overline{e}_w^{n+\frac12}})\|_{L^2}=C\|\nabla\overline{e}_w^{n+\frac12}\|_{L^2},
$$

we arrive at

$$
\begin{aligned}
I_{1,3}=&\big(\widetilde{\phi}^{n+\frac12}\overline{\boldsymbol{u}}^{n+\frac12}-Q_h\widetilde{\phi}^{n+\frac12}\overline{\boldsymbol{u}}^{n+\frac12},\nabla\overline{e}_w^{n+\frac12}\big)+\big(Q_h\widetilde{\phi}^{n+\frac12}\overline{\boldsymbol{u}}^{n+\frac12}-\widetilde{\phi}_h^{n+\frac12}\overline{\boldsymbol{u}}^{n+\frac12},\nabla\overline{e}_w^{n+\frac12}\big)\\
&+\big(\widetilde{\phi}_h^{n+\frac12}\overline{\boldsymbol{u}}^{n+\frac12}-\widetilde{\phi}_h^{n+\frac12}\boldsymbol{R}_h\overline{\boldsymbol{u}}^{n+\frac12},\nabla\overline{e}_w^{n+\frac12}\big)+\big(\widetilde{\phi}_h^{n+\frac12}\boldsymbol{R}_h\overline{\boldsymbol{u}}^{n+\frac12}-\widetilde{\phi}_h^{n+\frac12}\overline{\boldsymbol{u}}_h^{n+\frac12},\nabla\overline{e}_w^{n+\frac12}\big)\\
\le&\|\widetilde{\phi}^{n+\frac12}-Q_h\widetilde{\phi}^{n+\frac12}\|_{L^2}\|\overline{\boldsymbol{u}}^{n+\frac12}\|_{L^\infty}\|\nabla\overline{e}_w^{n+\frac12}\|_{L^2}+\big(\widetilde{e}_\phi^{n+\frac12}\overline{\boldsymbol{u}}^{n+\frac12},\nabla(\overline{e}_w^{n+\frac12}-\overline{\overline{e}_w^{n+\frac12}})\big)\\
&+\|\widetilde{\phi}_h^{n+\frac12}\|_{L^\infty}\|\overline{\boldsymbol{u}}_h^{n+\frac12}-\boldsymbol{R}_h\overline{\boldsymbol{u}}_h^{n+\frac12}\|_{L^2}\|\nabla\overline{e}_w^{n+\frac12}\|_{L^2}+\big(\widetilde{\phi}_h^{n+\frac12}\overline{e}_{\boldsymbol{u}}^{n+\frac12},\nabla\overline{e}_w^{n+\frac12}\big)\\
\le&Ch^{r+1}\|\nabla\overline{e}_w^{n+\frac12}\|_{L^2}+|\big(\nabla\widetilde{e}_\phi^{n+\frac12}\overline{\boldsymbol{u}}^{n+\frac12},\overline{e}_w^{n+\frac12}-\overline{\overline{e}_w^{n+\frac12}}\big)|+\big(\widetilde{\phi}_h^{n+\frac12}\overline{e}_{\boldsymbol{u}}^{n+\frac12},\nabla\overline{e}_w^{n+\frac12}\big)\\
\le&Ch^{r+1}\|\nabla\overline{e}_w^{n+\frac12}\|_{L^2}+\|\nabla\widetilde{e}_\phi^{n+\frac12}\|_{L^2}\|\overline{\boldsymbol{u}}^{n+\frac12}\|_{L^\infty}\|\overline{e}_w^{n+\frac12}-\overline{\overline{e}_w^{n+\frac12}}\|_{L^2}+\big(\widetilde{\phi}_h^{n+\frac12}\overline{e}_{\boldsymbol{u}}^{n+\frac12},\nabla\overline{e}_w^{n+\frac12}\big)\\
\le&C(h^{2r+2}+\|\nabla\widetilde{e}_\phi^{n+\frac12}\|_{L^2}^2)+\frac{\varepsilon}{4}\|\nabla\overline{e}_w^{n+\frac12}\|_{L^2}^2+\big(\widetilde{\phi}_h^{n+\frac12}\overline{e}_{\boldsymbol{u}}^{n+\frac12},\nabla\overline{e}_w^{n+\frac12}\big),
\end{aligned}
$$

where we have used (42), (44), Lemma 4.4, and integration in parts in the second inequality. In view of the truncation error terms and using the mass conservation of ϕ, $I_{1,4}$ can be bounded by

$$
\begin{aligned}
I_{1,4}=&\big(\delta_\tau Q_h\phi^{n+\frac12}-\delta_\tau\phi^{n+\frac12},\overline{e}_w^{n+\frac12}-\overline{\overline{e}_w^{n+\frac12}}\big)+\big(\delta_\tau\phi^{n+\frac12}-\phi_t^{n+\frac12},\overline{e}_w^{n+\frac12}-\overline{\overline{e}_w^{n+\frac12}}\big)\\
&+\varepsilon\big(\nabla(\overline{w}^{n+\frac12}-w^{n+\frac12}),\nabla\overline{e}_w^{n+\frac12}\big)-\big(\widetilde{\phi}^{n+\frac12}\overline{\boldsymbol{u}}^{n+\frac12}-\phi^{n+\frac12}\boldsymbol{u}^{n+\frac12},\nabla\overline{e}_w^{n+\frac12}\big)\\
\le&\|Q_h\delta_\tau\phi^{n+\frac12}-\delta_\tau\phi^{n+\frac12}\|_{L^2}\|\overline{e}_w^{n+\frac12}-\overline{\overline{e}_w^{n+\frac12}}\|_{L^2}+\|\delta_\tau\phi^{n+\frac12}-\phi_t^{n+\frac12}\|_{L^2}\|\overline{e}_w^{n+\frac12}-\overline{\overline{e}_w^{n+\frac12}}\|_{L^2}\\
&+\varepsilon\|\nabla(\overline{w}^{n+\frac12}-w^{n+\frac12})\|_{L^2}\|\nabla\overline{e}_w^{n+\frac12}\|_{L^2}+\|\widetilde{\phi}^{n+\frac12}\overline{\boldsymbol{u}}^{n+\frac12}-\phi^{n+\frac12}\boldsymbol{u}^{n+\frac12}\|_{L^2}\|\nabla\overline{e}_w^{n+\frac12}\|_{L^2}\\
\le&C(h^{2r}+\tau^4)+\frac{\varepsilon}{4}\|\nabla\overline{e}_w^{n+\frac12}\|_{L^2}^2.
\end{aligned}
$$

By using (51) again, it is clear to see that

$$
I_{1,5}\le C(h^{2r}+\tau^4)+\zeta\|\delta_\tau e_\phi^{n+\frac12}\|_{-1,h}^2.
$$

Combining the estimates of $I_{1,i}$, $1 \le i \le 5$, (63) becomes

$$\begin{aligned}&\frac{\varepsilon}{2\tau}(\|\nabla e_\phi^{n+1}\|_{L^2}^2 - \|\nabla e_\phi^n\|_{L^2}^2) + \frac{\varepsilon}{2}\|\nabla \overline{e}_w^{n+\frac12}\|_{L^2}^2 + \frac{\varepsilon}{8\tau}(\|\nabla(e_\phi^{n+1} - e_\phi^n)\|_{L^2}^2 - \|\nabla(e_\phi^n - e_\phi^{n-1})\|_{L^2}^2)\\ &\le C(h^{2r} + \tau^4 + \|\nabla e_\phi^{n+1}\|_{L^2}^2 + \|\nabla e_\phi^n\|_{L^2}^2) + \zeta\|\delta_\tau e_\phi^{n+\frac12}\|_{-1,h}^2 + \big(\widetilde{\phi}_h^{n+\frac12}\overline{e}_{\boldsymbol{u}}^{n+\frac12}, \nabla \overline{e}_w^{n+\frac12}\big). \end{aligned} \tag{64}$$

<u>*Step 2:*</u> By taking $\boldsymbol{v}_h = \overline{e}_{\boldsymbol{u}}^{n+\frac12}$ in (60) and $q_h = \overline{e}_p^{n+\frac12}$ in (62), we get

$$\begin{aligned}&\frac{1}{2\tau}(\|e_{\boldsymbol{u}}^{n+1}\|_{L^2}^2 - \|e_{\boldsymbol{u}}^n\|_{L^2}^2) + \eta\|\nabla \overline{e}_{\boldsymbol{u}}^{n+\frac12}\|_{L^2}^2\\ &= -\big[b\big(\widetilde{\boldsymbol{u}}^{n+\frac12}, \overline{\boldsymbol{u}}^{n+\frac12}, \overline{e}_{\boldsymbol{u}}^{n+\frac12}\big) - b\big(\widetilde{\boldsymbol{u}}_h^{n+\frac12}, \overline{\boldsymbol{u}}_h^{n+\frac12}, \overline{e}_{\boldsymbol{u}}^{n+\frac12}\big)\big] - \lambda\big(\widetilde{\phi}^{n+\frac12}\nabla\overline{w}^{n+\frac12} - \widetilde{\phi}_h^{n+\frac12}\nabla\overline{w}_h^{n+\frac12}, \overline{e}_{\boldsymbol{u}}^{n+\frac12}\big)\\ &\quad + \mu\big((\nabla\times\overline{\boldsymbol{B}}^{n+\frac12})\times\widetilde{\boldsymbol{B}}^{n+\frac12} - (\nabla\times\overline{\boldsymbol{B}}_h^{n+\frac12})\times\widetilde{\boldsymbol{B}}_h^{n+\frac12}, \overline{e}_{\boldsymbol{u}}^{n+\frac12}\big) + T_{\boldsymbol{u}}(\overline{e}_{\boldsymbol{u}}^{n+\frac12})\\ &:= \sum_{i=1}^4 I_{2,i}. \end{aligned} \tag{65}$$

Now, we start to estimate the right-hand side of (65). By (21), we can rewrite $I_{2,1}$ as follows:

$$\begin{aligned}|I_{2,1}| &= \Big| - b\big(\widetilde{\boldsymbol{u}}^{n+\frac12}, \overline{\boldsymbol{u}}^{n+\frac12} - \boldsymbol{R}_h\overline{\boldsymbol{u}}^{n+\frac12}, \overline{e}_{\boldsymbol{u}}^{n+\frac12}\big) + b\big(\widetilde{\boldsymbol{u}}^{n+\frac12} - \boldsymbol{R}_h\widetilde{\boldsymbol{u}}^{n+\frac12}, \overline{\boldsymbol{u}}^{n+\frac12} - \boldsymbol{R}_h\overline{\boldsymbol{u}}^{n+\frac12}, \overline{e}_{\boldsymbol{u}}^{n+\frac12}\big)\\ &\quad - b\big(\widetilde{\boldsymbol{u}}^{n+\frac12} - \boldsymbol{R}_h\widetilde{\boldsymbol{u}}^{n+\frac12}, \overline{\boldsymbol{u}}^{n+\frac12}, \overline{e}_{\boldsymbol{u}}^{n+\frac12}\big) + b\big(\widetilde{e}_{\boldsymbol{u}}^{n+\frac12}, \overline{\boldsymbol{u}}^{n+\frac12} - \boldsymbol{R}_h\overline{\boldsymbol{u}}^{n+\frac12}, \overline{e}_{\boldsymbol{u}}^{n+\frac12}\big)\\ &\quad - b\big(\widetilde{e}_{\boldsymbol{u}}^{n+\frac12}, \overline{\boldsymbol{u}}^{n+\frac12}, \overline{e}_{\boldsymbol{u}}^{n+\frac12}\big) - b\big(\widetilde{\boldsymbol{u}}_h^{n+\frac12}, \overline{e}_{\boldsymbol{u}}^{n+\frac12}, \overline{e}_{\boldsymbol{u}}^{n+\frac12}\big)\Big|\\ &\le C\|\widetilde{\boldsymbol{u}}^{n+\frac12}\|_{L^3}\|\nabla(\overline{\boldsymbol{u}}^{n+\frac12} - \boldsymbol{R}_h\overline{\boldsymbol{u}}^{n+\frac12})\|_{L^2}\|\nabla\overline{e}_{\boldsymbol{u}}^{n+\frac12}\|_{L^2}\\ &\quad + C\|\widetilde{\boldsymbol{u}}^{n+\frac12} - \boldsymbol{R}_h\widetilde{\boldsymbol{u}}^{n+\frac12}\|_{L^3}\|\nabla(\overline{\boldsymbol{u}}^{n+\frac12} - \boldsymbol{R}_h\overline{\boldsymbol{u}}^{n+\frac12})\|_{L^2}\|\nabla\overline{e}_{\boldsymbol{u}}^{n+\frac12}\|_{L^2}\\ &\quad + C\|\widetilde{\boldsymbol{u}}^{n+\frac12} - \boldsymbol{R}_h\widetilde{\boldsymbol{u}}^{n+\frac12}\|_{L^2}\|\overline{\boldsymbol{u}}^{n+\frac12}\|_{W^{1,4}}\|\nabla\overline{e}_{\boldsymbol{u}}^{n+\frac12}\|_{L^2}\\ &\quad + C\|\widetilde{e}_{\boldsymbol{u}}^{n+\frac12}\|_{L^2}\|\overline{\boldsymbol{u}}^{n+\frac12} - \boldsymbol{R}_h\overline{\boldsymbol{u}}^{n+\frac12}\|_{W^{1,4}}\|\nabla\overline{e}_{\boldsymbol{u}}^{n+\frac12}\|_{L^2}\\ &\quad + C\|\widetilde{e}_{\boldsymbol{u}}^{n+\frac12}\|_{L^2}\|\overline{\boldsymbol{u}}^{n+\frac12}\|_{W^{1,4}}\|\nabla\overline{e}_{\boldsymbol{u}}^{n+\frac12}\|_{L^2}\\ &\le C(h^{2r} + \|\widetilde{e}_{\boldsymbol{u}}^{n+\frac12}\|_{L^2}^2) + \frac{\eta}{8}\|\nabla\overline{e}_{\boldsymbol{u}}^{n+\frac12}\|_{L^2}^2, \end{aligned}$$

where we have used (43)–(44) and the identity $b\big(\widetilde{\boldsymbol{u}}_h^{n+\frac12}, \overline{e}_{\boldsymbol{u}}^{n+\frac12}, \overline{e}_{\boldsymbol{u}}^{n+\frac12}\big) = 0$. To estimate $I_{2,2}$, we define the spatial mass average

$$\begin{aligned}\overline{\widetilde{e}_\phi^{n+\frac12}} = |\Omega|^{-1}(\widetilde{e}_\phi{}^{n+\frac12}, 1) = |\Omega|^{-1}(Q_h\widetilde{\phi}^{n+\frac12} - \widetilde{\phi}_h^{n+\frac12}, 1) &= |\Omega|^{-1}(\widetilde{\phi}^{n+\frac12} - \widetilde{\phi}_h^{n+\frac12}, 1)\\ &= |\Omega|^{-1}(\phi^0 - \phi_h^0, 1), \end{aligned}$$

which implies that

$$\Big|\overline{\widetilde{e}_\phi^{n+\frac12}}\Big| \le Ch^{r+1}.$$

Then, $I_{2,2}$ can be bounded by

$$\begin{aligned}I_{2,2} =& -\lambda\Big[\big((\widetilde{\phi}^{n+\frac12} - Q_h\widetilde{\phi}^{n+\frac12})\nabla\overline{w}^{n+\frac12}, \overline{e}_{\boldsymbol{u}}^{n+\frac12}\big) + \big(\widetilde{e}_\phi^{n+\frac12}\nabla\overline{w}^{n+\frac12}, \overline{e}_{\boldsymbol{u}}^{n+\frac12}\big)\\ &+ \big(\widetilde{\phi}_h^{n+\frac12}\nabla(\overline{w}^{n+\frac12} - Q_h\overline{w}^{n+\frac12}), \overline{e}_{\boldsymbol{u}}^{n+\frac12}\big) + \big(\widetilde{\phi}_h^{n+\frac12}\nabla\overline{e}_w^{n+\frac12}, \overline{e}_{\boldsymbol{u}}^{n+\frac12}\big)\Big]\\ \le& C(\|\widetilde{\phi}^{n+\frac12} - Q_h\widetilde{\phi}^{n+\frac12}\|_{L^2}\|\nabla\overline{w}^{n+\frac12}\|_{L^\infty}\|\overline{e}_{\boldsymbol{u}}^{n+\frac12}\|_{L^2} + |\big(\widetilde{e}_\phi^{n+\frac12}\nabla\overline{w}^{n+\frac12}, \overline{e}_{\boldsymbol{u}}^{n+\frac12}\big)|\\ &+ \|\widetilde{\phi}_h^{n+\frac12}\|_{L^\infty}\|\nabla(\overline{w}^{n+\frac12} - Q_h\overline{w}^{n+\frac12})\|_{L^2}\|\overline{e}_{\boldsymbol{u}}^{n+\frac12}\|_{L^2}) - \lambda\big(\widetilde{\phi}_h^{n+\frac12}\nabla\overline{e}_w^{n+\frac12}, \overline{e}_{\boldsymbol{u}}^{n+\frac12}\big)\\ \le& C(h^{2r} + \|\overline{e}_{\boldsymbol{u}}^{n+\frac12}\|_{L^2}^2 + \|\nabla\widetilde{e}_\phi^{n+\frac12}\|_{L^2}^2) + \frac{\eta}{8}\|\nabla\overline{e}_{\boldsymbol{u}}^{n+\frac12}\|_{L^2}^2 - \lambda\big(\widetilde{\phi}_h^{n+\frac12}\nabla\overline{e}_w^{n+\frac12}, \overline{e}_{\boldsymbol{u}}^{n+\frac12}\big), \end{aligned}$$

where we have used (42) and the following inequality:

$$\begin{aligned}
&\Big| -(\widetilde{e}_\phi^{n+\frac12}\nabla \overline{w}^{n+\frac12}, \overline{e}_{\boldsymbol u}^{n+\frac12})\Big| \\
&= |(\nabla \widetilde{e}_\phi^{n+\frac12}\overline{w}^{n+\frac12}, \overline{e}_{\boldsymbol u}^{n+\frac12}) + (\widetilde{e}_\phi^{n+\frac12}\overline{w}^{n+\frac12}, \nabla\cdot \overline{e}_{\boldsymbol u}^{n+\frac12})| \\
&\le \|\nabla \widetilde{e}_\phi^{n+\frac12}\|_{L^2}\|\overline{w}^{n+\frac12}\|_{L^2}\ \|_{L^\infty}\ \|\overline{e}_{\boldsymbol u}^{n+\frac12}\|_{L^2} + \|\widetilde{e}_\phi^{n+\frac12} - \overline{\widetilde{e}_\phi^{n+\frac12}}\|_{L^2}\|\overline{w}^{n+\frac12}\|_{L^\infty}\|\nabla\cdot \overline{e}_{\boldsymbol u}^{n+\frac12}\|_{L^2} \\
&\quad + \|\overline{\widetilde{e}_\phi^{n+\frac12}}\|_{L^2}\|\overline{w}^{n+\frac12}\|_{L^\infty}\|\nabla\cdot \overline{e}_{\boldsymbol u}^{n+\frac12}\|_{L^2} \\
&\le C(\|\nabla \widetilde{e}_\phi^{n+\frac12}\|_{L^2}^2 + \|\overline{e}_{\boldsymbol u}^{n+\frac12}\|_{L^2}^2 + h^{2r+2}) + \frac{\eta}{16}\|\nabla \overline{e}_{\boldsymbol u}^{n+\frac12}\|_{L^2}^2.
\end{aligned}$$

For $I_{2,3}$, we see that

$$\begin{aligned}
I_{2,3} =&\mu\Big[\big((\nabla\times\overline{\boldsymbol B}^{n+\frac12})\times\widetilde{\boldsymbol B}^{n+\frac12} - (\nabla\times\overline{\boldsymbol B}^{n+\frac12})\times\Pi_h\widetilde{\boldsymbol B}^{n+\frac12}, \overline{e}_{\boldsymbol u}^{n+\frac12}\big) \\
&+\big((\nabla\times\overline{\boldsymbol B}^{n+\frac12})\times\Pi_h\widetilde{\boldsymbol B}^{n+\frac12} - (\nabla\times\overline{\boldsymbol B}^{n+\frac12})\times\widetilde{\boldsymbol B}_h^{n+\frac12}, \overline{e}_{\boldsymbol u}^{n+\frac12}\big) \\
&+\big((\nabla\times\overline{\boldsymbol B}^{n+\frac12})\times\widetilde{\boldsymbol B}_h^{n+\frac12} - (\nabla\times\Pi_h\overline{\boldsymbol B}^{n+\frac12})\times\widetilde{\boldsymbol B}_h^{n+\frac12}, \overline{e}_{\boldsymbol u}^{n+\frac12}\big) \\
&+\big((\nabla\times\Pi_h\overline{\boldsymbol B}^{n+\frac12})\times\widetilde{\boldsymbol B}_h^{n+\frac12} - (\nabla\times\overline{\boldsymbol B}_h^{n+\frac12})\times\widetilde{\boldsymbol B}_h^{n+\frac12}, \overline{e}_{\boldsymbol u}^{n+\frac12}\big)\Big] \\
\le&\mu(\|\nabla\times\overline{\boldsymbol B}^{n+\frac12}\|_{L^\infty}\|\widetilde{\boldsymbol B}^{n+\frac12} - \Pi_h\widetilde{\boldsymbol B}^{n+\frac12}\|_{L^2}\|\overline{e}_{\boldsymbol u}^{n+\frac12}\|_{L^2} + \|\nabla\times\overline{\boldsymbol B}^{n+\frac12}\|_{L^\infty}\|\widetilde{e}_{\boldsymbol B}^{n+\frac12}\|_{L^2}\|\overline{e}_{\boldsymbol u}^{n+\frac12}\|_{L^2}) \\
&+\mu\big((\nabla\times(\overline{\boldsymbol B}^{n+\frac12} - \Pi_h\overline{\boldsymbol B}^{n+\frac12}))\times\widetilde{\boldsymbol B}_h^{n+\frac12}, \overline{e}_{\boldsymbol u}^{n+\frac12}\big) + \mu\big((\nabla\times\overline{e}_{\boldsymbol B}^{n+\frac12})\times\widetilde{\boldsymbol B}_h^{n+\frac12}, \overline{e}_{\boldsymbol u}^{n+\frac12}\big) \\
\le&C(h^{2r} + \|\overline{e}_{\boldsymbol u}^{n+\frac12}\|_{L^2}^2 + \|\widetilde{e}_{\boldsymbol B}^{n+\frac12}\|_{L^2}^2) + \frac{\eta}{8}\|\overline{e}_{\boldsymbol u}^{n+\frac12}\|_{H^1}^2 + \mu\big((\nabla\times\overline{e}_{\boldsymbol B}^{n+\frac12})\times\widetilde{\boldsymbol B}_h^{n+\frac12}, \overline{e}_{\boldsymbol u}^{n+\frac12}\big),
\end{aligned}$$

where we have used the projection estimate (46) and the following inequality

$$\begin{aligned}
&\mu\big((\nabla\times(\overline{\boldsymbol B}^{n+\frac12} - \Pi_h\overline{\boldsymbol B}^{n+\frac12}))\times\widetilde{\boldsymbol B}_h^{n+\frac12}, \overline{e}_{\boldsymbol u}^{n+\frac12}\big) \\
&= -\mu\big((\nabla\times(\overline{\boldsymbol B}^{n+\frac12} - \Pi_h\overline{\boldsymbol B}^{n+\frac12}))\times\widetilde{e}_{\boldsymbol B}^{n+\frac12}, \overline{e}_{\boldsymbol u}^{n+\frac12}\big) \\
&\quad + \mu\big((\nabla\times(\overline{\boldsymbol B}^{n+\frac12} - \Pi_h\overline{\boldsymbol B}^{n+\frac12}))\times\Pi_h\widetilde{\boldsymbol B}^{n+\frac12}, \overline{e}_{\boldsymbol u}^{n+\frac12}\big) \\
&\le \|\nabla\times(\overline{\boldsymbol B}^{n+\frac12} - \Pi_h\overline{\boldsymbol B}^{n+\frac12})\|_{L^3}\|\widetilde{e}_{\boldsymbol B}^{n+\frac12}\|_{L^2}\|\overline{e}_{\boldsymbol u}^{n+\frac12}\|_{L^6} \\
&\quad + \|\nabla\times(\overline{\boldsymbol B}^{n+\frac12} - \Pi_h\overline{\boldsymbol B}^{n+\frac12})\|_{L^2}\|\Pi_h\widetilde{\boldsymbol B}^{n+\frac12}\|_{L^3}\|\overline{e}_{\boldsymbol u}^{n+\frac12}\|_{L^6} \\
&\le C(\|\widetilde{e}_{\boldsymbol B}^{n+\frac12}\|_{L^2}^2 + Ch^{2r}) + \frac{\eta}{8}\|\overline{e}_{\boldsymbol u}^{n+\frac12}\|_{H^1}^2.
\end{aligned}$$

By using Taylor expansion and projection estimate (44), the truncation error term $I_{2,4}$ can be bounded by

$$I_{2,4} \le C(h^{2r} + \tau^4) + \frac{\eta}{8}\|\nabla \overline{e}_{\boldsymbol u}^{n+\frac12}\|_{L^2}^2.$$

Combining the estimates of $I_{2,i}$, $1 \le i \le 4$, (65) becomes

$$\begin{aligned}
&\frac{1}{2\tau}(\|e_{\boldsymbol u}^{n+1}\|_{L^2}^2 - \|e_{\boldsymbol u}^{n}\|_{L^2}^2) + \frac{\eta}{2}\|\nabla \overline{e}_{\boldsymbol u}^{n+\frac12}\|_{L^2}^2 \\
&\le C(h^{2r} + \tau^4 + \|\overline{e}_{\boldsymbol u}^{n+\frac12}\|_{L^2}^2 + \|\overline{e}_{\boldsymbol u}^{n+\frac12}\|_{L^2}^2 + \|\nabla e_\phi^{n+1}\|_{L^2}^2 + \|\nabla e_\phi^{n}\|_{L^2}^2 + \|\nabla e_\phi^{n-1}\|_{L^2}^2 + \|\widetilde{e}_{\boldsymbol B}^{n+\frac12}\|_{L^2}^2) \\
&\quad - \lambda\big(\widetilde{\phi}_h^{n+\frac12}\nabla \overline{e}_w^{n+\frac12}, \overline{e}_{\boldsymbol u}^{n+\frac12}\big) + \mu\big((\nabla\times\overline{e}_{\boldsymbol B}^{n+\frac12})\times\widetilde{\boldsymbol B}_h^{n+\frac12}, \overline{e}_{\boldsymbol u}^{n+\frac12}\big).
\end{aligned} \tag{66}$$

Step 3: A substitution of $\boldsymbol l_h = \overline{e}_{\boldsymbol B}^{n+\frac12}$ in (61) gives

$$\begin{aligned}
&\frac{\mu}{2\tau}(\|e_{\boldsymbol B}^{n+1}\|_{L^2} - \|e_{\boldsymbol B}^{n}\|_{L^2}^2) + \sigma^{-1}\|\nabla\times\overline{e}_{\boldsymbol B}^{n+\frac12}\|_{L^2}^2 + \sigma^{-1}\|\nabla\cdot\overline{e}_{\boldsymbol B}^{n+\frac12}\|_{L^2}^2 \\
&= \mu\big(\overline{\boldsymbol u}^{n+\frac12}\times\widetilde{\boldsymbol B}^{n+\frac12} - \overline{\boldsymbol u}_h^{n+\frac12}\times\widetilde{\boldsymbol B}_h^{n+\frac12}, \nabla\times\overline{e}_{\boldsymbol B}^{n+\frac12}\big) + T_{\boldsymbol B}(\overline{e}_{\boldsymbol B}^{n+\frac12}) \\
&:= \sum_{i=1}^{2} I_{3,i}.
\end{aligned} \tag{67}$$

For the right-hand side of (67), $I_{3,1}$ can be controlled by

$$
\begin{aligned}
I_{3,1} =&\mu\big[\big(\overline{\boldsymbol{u}}^{n+\frac12}\times(\widetilde{\boldsymbol{B}}^{n+\frac12}-\Pi_h\widetilde{\boldsymbol{B}}^{n+\frac12}),\nabla\times\overline{e}_{\boldsymbol{B}}^{n+\frac12}\big)+\big(\overline{\boldsymbol{u}}^{n+\frac12}\times\widetilde{e}_{\boldsymbol{B}}^{n+\frac12},\nabla\times\overline{e}_{\boldsymbol{B}}^{n+\frac12}\big)\\
&+\big((\overline{\boldsymbol{u}}^{n+\frac12}-\boldsymbol{R}_h\overline{\boldsymbol{u}}^{n+\frac12})\times\widetilde{\boldsymbol{B}}_h^{n+\frac12},\nabla\times\overline{e}_{\boldsymbol{B}}^{n+\frac12}\big)+\big(\overline{e}_{\boldsymbol{u}}^{n+\frac12}\times\widetilde{\boldsymbol{B}}_h^{n+\frac12},\nabla\times\overline{e}_{\boldsymbol{B}}^{n+\frac12}\big)\big]\\
\le&\mu\|\overline{\boldsymbol{u}}^{n+\frac12}\|_{L^\infty}\|\widetilde{\boldsymbol{B}}^{n+\frac12}-\Pi_h\widetilde{\boldsymbol{B}}^{n+\frac12}\|_{L^2}\|\nabla\times\overline{e}_{\boldsymbol{B}}^{n+\frac12}\|_{L^2}+\|\overline{\boldsymbol{u}}^{n+\frac12}\|_{L^\infty}\|\widetilde{e}_{\boldsymbol{B}}^{n+\frac12}\|_{L^2}\|\nabla\times\overline{e}_{\boldsymbol{B}}^{n+\frac12}\|_{L^2}\\
&+C(\|\widetilde{e}_{\boldsymbol{B}}^{n+\frac12}\|_{L^2}^2+h^{2r})+\frac{\sigma^{-1}}{12}\|\nabla\times\overline{e}_{\boldsymbol{B}}^{n+\frac12}\|_{L^2}^2+\mu\big(\overline{e}_{\boldsymbol{u}}^{n+\frac12}\times\widetilde{\boldsymbol{B}}_h^{n+\frac12},\nabla\times\overline{e}_{\boldsymbol{B}}^{n+\frac12}\big)\\
\le&C(h^{2r}+\|\widetilde{e}_{\boldsymbol{B}}^{n+\frac12}\|_{L^2}^2)+\frac{\sigma^{-1}}{4}\|\nabla\times\overline{e}_{\boldsymbol{B}}^{n+\frac12}\|_{L^2}^2+\mu\big(\overline{e}_{\boldsymbol{u}}^{n+\frac12}\times\widetilde{\boldsymbol{B}}_h^{n+\frac12},\nabla\times\overline{e}_{\boldsymbol{B}}^{n+\frac12}\big),
\end{aligned}
$$

where we have used (46) and the following inequality

$$
\begin{aligned}
&\mu((\overline{\boldsymbol{u}}^{n+\frac12}-\boldsymbol{R}_h\overline{\boldsymbol{u}}^{n+\frac12})\times\widetilde{\boldsymbol{B}}_h^{n+\frac12},\nabla\times\overline{e}_{\boldsymbol{B}}^{n+\frac12})\\
&=-\mu((\overline{\boldsymbol{u}}^{n+\frac12}-\boldsymbol{R}_h\overline{\boldsymbol{u}}^{n+\frac12})\times\widetilde{e}_{\boldsymbol{B}}^{n+\frac12},\nabla\times\overline{e}_{\boldsymbol{B}}^{n+\frac12})+\mu((\overline{\boldsymbol{u}}^{n+\frac12}-\boldsymbol{R}_h\overline{\boldsymbol{u}}^{n+\frac12})\times\Pi_h\widetilde{\boldsymbol{B}}^{n+\frac12},\nabla\times\overline{e}_{\boldsymbol{B}}^{n+\frac12})\\
&\le\mu\|\overline{\boldsymbol{u}}^{n+\frac12}-\boldsymbol{R}_h\overline{\boldsymbol{u}}^{n+\frac12}\|_{L^\infty}\|\widetilde{e}_{\boldsymbol{B}}^{n+\frac12}\|_{L^2}\|\nabla\times\overline{e}_{\boldsymbol{B}}^{n+\frac12}\|_{L^2}\\
&\quad+\mu\|\overline{\boldsymbol{u}}^{n+\frac12}-\boldsymbol{R}_h\overline{\boldsymbol{u}}^{n+\frac12}\|_{L^6}\|\Pi_h\widetilde{\boldsymbol{B}}^{n+\frac12}\|_{L^3}\|\nabla\times\overline{e}_{\boldsymbol{B}}^{n+\frac12}\|_{L^2}\\
&\le C(\|\widetilde{e}_{\boldsymbol{B}}^{n+\frac12}\|_{L^2}^2+h^{2r})+\frac{\sigma^{-1}}{12}\|\nabla\times\overline{e}_{\boldsymbol{B}}^{n+\frac12}\|_{L^2}^2\quad\text{(here use (43)–(44))}.
\end{aligned}
$$

By using Taylor expansions again, we further get

$$
I_{3,2}\le C(h^{2r}+\tau^4+\|\overline{e}_{\boldsymbol{B}}^{n+\frac12}\|_{L^2}^2)+\frac{\sigma^{-1}}{4}\|\nabla\times\overline{e}_{\boldsymbol{B}}^{n+\frac12}\|_{L^2}^2+\frac{\sigma^{-1}}{4}\|\nabla\cdot\overline{e}_{\boldsymbol{B}}^{n+\frac12}\|_{L^2}^2.
$$

Combining the estimates of $I_{3,1}$ and $I_{3,2}$, (67) becomes

$$
\begin{aligned}
&\frac{\mu}{2\tau}(\|e_{\boldsymbol{B}}^{n+1}\|_{L^2}^2-\|e_{\boldsymbol{B}}^{n}\|_{L^2}^2)+\frac{\sigma^{-1}}{2}\|\nabla\times\overline{e}_{\boldsymbol{B}}^{n+\frac12}\|_{L^2}^2+\frac{3\sigma^{-1}}{4}\|\nabla\cdot\overline{e}_{\boldsymbol{B}}^{n+\frac12}\|_{L^2}^2\\
&\le C(h^{2r}+\tau^4+\|\widetilde{e}_{\boldsymbol{B}}^{n+\frac12}\|_{L^2}^2+\|\overline{e}_{\boldsymbol{B}}^{n+\frac12}\|_{L^2}^2)+\mu\big(\overline{e}_{\boldsymbol{u}}^{n+\frac12}\times\widetilde{\boldsymbol{B}}_h^{n+\frac12},\nabla\times\overline{e}_{\boldsymbol{B}}^{n+\frac12}\big).
\end{aligned}
\tag{68}
$$

Step 4: Finally, a summation of (64), (66) and (68) gives

$$
\begin{aligned}
&\frac{\lambda\varepsilon}{2\tau}(\|\nabla e_\phi^{n+1}\|_{L^2}^2-\|\nabla e_\phi^{n}\|_{L^2}^2)+\frac{\lambda\varepsilon}{8\tau}(\|\nabla(e_\phi^{n+1}-e_\phi^{n})\|_{L^2}^2-\|\nabla(e_\phi^{n}-e_\phi^{n-1})\|_{L^2}^2)\\
&\quad+\frac{1}{2\tau}(\|e_{\boldsymbol{u}}^{n+1}\|_{L^2}^2-\|e_{\boldsymbol{u}}^{n}\|_{L^2}^2)+\frac{\mu}{2\tau}(\|e_{\boldsymbol{B}}^{n+1}\|_{L^2}^2-\|e_{\boldsymbol{B}}^{n}\|_{L^2}^2)+\frac{\eta}{2}\|\nabla\overline{e}_{\boldsymbol{u}}^{n+\frac12}\|_{L^2}^2\\
&\quad+\frac{\lambda\varepsilon}{2}\|\nabla\overline{e}_w^{n+\frac12}\|_{L^2}^2+\frac{\sigma^{-1}}{2}\|\nabla\times\overline{e}_{\boldsymbol{B}}^{n+\frac12}\|_{L^2}^2+\frac{3\sigma^{-1}}{4}\|\nabla\cdot\overline{e}_{\boldsymbol{B}}^{n+\frac12}\|_{L^2}^2\\
&\le C\Big(h^{2r}+\tau^4+\|\nabla e_\phi^{n+1}\|_{L^2}^2+\|\nabla e_\phi^{n}\|_{L^2}^2+\|\nabla e_\phi^{n-1}\|_{L^2}^2+\|\overline{e}_{\boldsymbol{u}}^{n+\frac12}\|_{L^2}^2+\|\widetilde{e}_{\boldsymbol{u}}^{n+\frac12}\|_{L^2}^2\\
&\quad+\|\overline{e}_{\boldsymbol{B}}^{n+\frac12}\|_{L^2}^2+\|\widetilde{e}_{\boldsymbol{B}}^{n+\frac12}\|_{L^2}^2\Big)+\zeta\|\delta_\tau e_\phi^{n+\frac12}\|_{-1,h}^2,
\end{aligned}
\tag{69}
$$

where ζ is an arbitrarily small positive constant. To complete the estimate of (69), it remains to analyze $\|\delta_\tau e_\phi^{n+\frac12}\|_{-1,h}^2$. To this end, we choose $\xi_h=T_h\delta_\tau e_\phi^{n+\frac12}$ in (58) and get

$$
\begin{aligned}
&\|\delta_\tau e_\phi^{n+\frac12}\|_{-1,h}^2=\big(\delta_\tau e_\phi^{n+\frac12},T_h\delta_\tau e_\phi^{n+\frac12}\big)\\
=&\big(\widetilde{\phi}^{n+\frac12}\overline{\boldsymbol{u}}^{n+\frac12}-\phi_h^{n+\frac12}\overline{\boldsymbol{u}}_h^{n+\frac12},\nabla T_h\delta_\tau e_\phi^{n+\frac12}\big)-\varepsilon\big(\nabla\overline{e}_w^{n+\frac12},\nabla T_h\delta_\tau e_\phi^{n+\frac12}\big)+T_\phi(T_h\delta_\tau e_\phi^{n+\frac12})\\
:=&\sum_{i=1}^{3}I_{4,i}.
\end{aligned}
\tag{70}
$$

Similarly, we define

$$
\overline{T_h\delta_\tau e_\phi^{n+\frac12}}:=|\Omega|^{-1}\big(T_h\delta_\tau e_\phi^{n+\frac12},1\big),
$$

and get $\|T_h\delta_\tau e_\phi^{n+\frac{1}{2}} - \overline{T_h\delta_\tau e_\phi^{n+\frac{1}{2}}}\|_{L^2} \le C\|\nabla T_h\delta_\tau e_\phi^{n+\frac{1}{2}}\|_{L^2}$. Then it is easy to derive

$$\begin{aligned}
I_{4,1} =&\big((\widetilde{\phi}^{n+\frac{1}{2}} - Q_h\widetilde{\phi}^{n+\frac{1}{2}})\overline{\boldsymbol{u}}^{n+\frac{1}{2}}, \nabla T_h\delta_\tau e_\phi^{n+\frac{1}{2}}\big) + \big(\widetilde{e}_\phi^{n+\frac{1}{2}}\overline{\boldsymbol{u}}^{n+\frac{1}{2}}, \nabla T_h\delta_\tau e_\phi^{n+\frac{1}{2}}\big)\\
&+ \big(\widetilde{\phi}_h^{n+\frac{1}{2}}(\overline{\boldsymbol{u}}^{n+\frac{1}{2}} - \boldsymbol{R}_h\overline{\boldsymbol{u}}^{n+\frac{1}{2}}), \nabla T_h\delta_\tau e_\phi^{n+\frac{1}{2}}\big) + \big(\widetilde{\phi}_h^{n+\frac{1}{2}}\overline{e}_{\boldsymbol{u}}^{n+\frac{1}{2}}, \nabla T_h\delta_\tau e_\phi^{n+\frac{1}{2}}\big)\\
\le&\|\widetilde{\phi}^{n+\frac{1}{2}} - Q_h\widetilde{\phi}^{n+\frac{1}{2}}\|_{L^2}\|\overline{\boldsymbol{u}}^{n+\frac{1}{2}}\|_{L^\infty}\|\nabla T_h\delta_\tau e_\phi^{n+\frac{1}{2}}\|_{L^2}\\
&+ \big|\big(\nabla\widetilde{e}_\phi^{n+\frac{1}{2}}\cdot\overline{\boldsymbol{u}}^{n+\frac{1}{2}}, T_h\delta_\tau e_\phi^{n+\frac{1}{2}} - \overline{T_h\delta_\tau e_\phi^{n+\frac{1}{2}}}\big)\big|\\
&+ \|\widetilde{\phi}_h^{n+\frac{1}{2}}\|_{L^\infty}\|\overline{\boldsymbol{u}}^{n+\frac{1}{2}} - \boldsymbol{R}_h\overline{\boldsymbol{u}}^{n+\frac{1}{2}}\|_{L^2}\|\nabla T_h\delta_\tau e_\phi^{n+\frac{1}{2}}\|_{L^2}\\
&+ \|\widetilde{\phi}_h^{n+\frac{1}{2}}\|_{L^\infty}\|\overline{e}_{\boldsymbol{u}}^{n+\frac{1}{2}}\|_{L^2}\|\nabla T_h\delta_\tau e_\phi^{n+\frac{1}{2}}\|_{L^2}\\
\le&C(h^{2r+2} + \|\nabla\widetilde{e}_\phi^{n+\frac{1}{2}}\|_{L^2}^2 + \|\overline{e}_{\boldsymbol{u}}^{n+\frac{1}{2}}\|_{L^2}^2) + \frac{1}{4}\|\nabla T_h\delta_\tau e_\phi^{n+\frac{1}{2}}\|_{L^2}^2,
\end{aligned}$$

where we have used integration by parts, $\nabla\cdot\boldsymbol{u} = 0$, and

$$\begin{aligned}
&\big|\big(\widetilde{e}_\phi^{n+\frac{1}{2}}\overline{\boldsymbol{u}}^{n+\frac{1}{2}}, \nabla T_h\delta_\tau e_\phi^{n+\frac{1}{2}}\big)\big|\\
=&\big|\big(\widetilde{e}_\phi^{n+\frac{1}{2}}\overline{\boldsymbol{u}}^{n+\frac{1}{2}}, \nabla(T_h\delta_\tau e_\phi^{n+\frac{1}{2}} - \overline{T_h\delta_\tau e_\phi^{n+\frac{1}{2}}})\big)\big|\\
=&\big|\big(\nabla\cdot(\widetilde{e}_\phi^{n+\frac{1}{2}}\overline{\boldsymbol{u}}^{n+\frac{1}{2}}), T_h\delta_\tau e_\phi^{n+\frac{1}{2}} - \overline{T_h\delta_\tau e_\phi^{n+\frac{1}{2}}}\big)\big|\\
=&\big|\big(\nabla\widetilde{e}_\phi^{n+\frac{1}{2}}\cdot\overline{\boldsymbol{u}}^{n+\frac{1}{2}}, T_h\delta_\tau e_\phi^{n+\frac{1}{2}} - \overline{T_h\delta_\tau e_\phi^{n+\frac{1}{2}}}\big) + \big(\widetilde{e}_\phi^{n+\frac{1}{2}}\nabla\cdot\overline{\boldsymbol{u}}^{n+\frac{1}{2}}, T_h\delta_\tau e_\phi^{n+\frac{1}{2}} - \overline{T_h\delta_\tau e_\phi^{n+\frac{1}{2}}}\big)\big|\\
=&\big|\big(\nabla\widetilde{e}_\phi^{n+\frac{1}{2}}\cdot\overline{\boldsymbol{u}}^{n+\frac{1}{2}}, T_h\delta_\tau e_\phi^{n+\frac{1}{2}} - \overline{T_h\delta_\tau e_\phi^{n+\frac{1}{2}}}\big)\big|.
\end{aligned}$$

Meanwhile, the estimate of $I_{4,2}$ is straightforward:

$$I_{4,2} \le C\|\nabla\overline{e}_w^{n+\frac{1}{2}}\|_{L^2}^2 + \frac{1}{4}\|\nabla T_h\delta_\tau e_\phi^{n+\frac{1}{2}}\|_{L^2}^2.$$

In view of the truncation error term $I_{4,3}$, we see that

$$\begin{aligned}
I_{4,3} =&\big(\delta_\tau Q_h\phi^{n+\frac{1}{2}} - \partial_t\phi^{n+\frac{1}{2}}, T_h\delta_\tau e_\phi^{n+\frac{1}{2}} - \overline{T_h\delta_\tau e_\phi^{n+\frac{1}{2}}}\big)\\
&+ \varepsilon\big(\nabla(\overline{w}^{n+\frac{1}{2}} - w^{n+\frac{1}{2}}), \nabla T_h\delta_\tau e_\phi^{n+\frac{1}{2}}\big),\\
&- \big(\widetilde{\phi}^{n+\frac{1}{2}}\overline{\boldsymbol{u}}^{n+\frac{1}{2}} - \phi^{n+\frac{1}{2}}\boldsymbol{u}^{n+\frac{1}{2}}, \nabla T_h\delta_\tau e_\phi^{n+\frac{1}{2}}\big)\\
\le&C(h^{2r} + \tau^4) + \frac{1}{4}\|\nabla T_h\delta_\tau e_\phi^{n+\frac{1}{2}}\|_{L^2}^2.
\end{aligned}$$

Combining the estimates of $I_{4,i}$, $1 \le i \le 3$, as well as the identity that $\|\nabla T_h\delta_\tau e_\phi^{n+\frac{1}{2}}\|_{L^2}^2 = \|\delta_\tau e_\phi^{n+\frac{1}{2}}\|_{-1,h}^2$, we obtain the following result from (70):

$$\|\delta_\tau e_\phi^{n+\frac{1}{2}}\|_{-1,h}^2 \le C(h^{2r} + \tau^4 + \|\nabla\widetilde{e}_\phi^{n+\frac{1}{2}}\|_{L^2}^2 + \|\overline{e}_{\boldsymbol{u}}^{n+\frac{1}{2}}\|_{L^2}^2 + \|\nabla\overline{e}_w^{n+\frac{1}{2}}\|_{L^2}^2). \tag{71}$$

Substituting the above estimate into (69), we get

$$\begin{aligned}
&\frac{\lambda\varepsilon}{2\tau}(\|\nabla e_\phi^{n+1}\|_{L^2}^2 - \|\nabla e_\phi^n\|_{L^2}^2) + \frac{\lambda\varepsilon}{8\tau}(\|\nabla(e_\phi^{n+1} - e_\phi^n)\|_{L^2}^2 - \|\nabla(e_\phi^n - e_\phi^{n-1})\|_{L^2}^2)\\
&\quad + \frac{1}{2\tau}(\|e_{\boldsymbol{u}}^{n+1}\|_{L^2}^2 - \|e_{\boldsymbol{u}}^n\|_{L^2}^2) + \frac{\mu}{2\tau}(\|e_{\boldsymbol{B}}^{n+1}\|_{L^2}^2 - \|e_{\boldsymbol{B}}^n\|_{L^2}^2) + \frac{\eta}{2}\|\nabla\overline{e}_{\boldsymbol{u}}^{n+\frac{1}{2}}\|_{L^2}^2\\
&\quad + \frac{\lambda\varepsilon}{4}\|\nabla\overline{e}_w^{n+\frac{1}{2}}\|_{L^2}^2 + \frac{\sigma^{-1}}{2}\|\nabla\times\overline{e}_{\boldsymbol{B}}^{n+\frac{1}{2}}\|_{L^2}^2 + \frac{3\sigma^{-1}}{4}\|\nabla\cdot\overline{e}_{\boldsymbol{B}}^{n+\frac{1}{2}}\|_{L^2}^2\\
&\le C\big(h^{2r} + \tau^4 + \|\nabla e_\phi^{n+1}\|_{L^2}^2 + \|\nabla e_\phi^n\|_{L^2}^2 + \|\nabla e_\phi^{n-1}\|_{L^2}^2 + \|\overline{e}_{\boldsymbol{u}}^{n+\frac{1}{2}}\|_{L^2}^2 + \|\widetilde{e}_{\boldsymbol{u}}^{n+\frac{1}{2}}\|_{L^2}^2\\
&\quad + \|\overline{e}_{\boldsymbol{B}}^{n+\frac{1}{2}}\|_{L^2}^2 + \|\widetilde{e}_{\boldsymbol{B}}^{n+\frac{1}{2}}\|_{L^2}^2\big).
\end{aligned} \tag{72}$$

Table 1
Temporal convergence for $\varepsilon = 1$ at $T = 0.5$.

τ	$\mathcal{E}(\nabla\phi)$	Order	$\mathcal{E}(\boldsymbol{u})$	Order	$\mathcal{E}(\boldsymbol{B})$	Order
1/18	1.109×10^{-3}		6.625×10^{-4}		6.169×10^{-4}	
1/36	3.110×10^{-4}	1.83	1.683×10^{-4}	1.98	1.561×10^{-4}	1.98
1/54	1.435×10^{-4}	1.91	7.504×10^{-5}	1.99	6.951×10^{-5}	2.00
1/72	8.232×10^{-5}	1.93	4.226×10^{-5}	2.00	3.913×10^{-5}	2.00
τ	$\mathcal{E}(\nabla w)$	Order	$\mathcal{E}(\nabla\boldsymbol{u})$	Order	$\mathcal{E}(\nabla\times\boldsymbol{B})$	Order
1/18	5.556×10^{-4}		3.025×10^{-4}		1.712×10^{-4}	
1/36	1.828×10^{-4}	1.60	7.627×10^{-5}	1.99	4.286×10^{-5}	2.00
1/54	8.806×10^{-5}	1.80	3.422×10^{-5}	1.98	1.907×10^{-5}	1.99
1/72	5.146×10^{-5}	1.87	1.967×10^{-5}	1.92	1.075×10^{-5}	1.99

By using the discrete Gronwall inequality, there exists a positive constant τ_0 such that when $\tau < \tau_0$,

$$\begin{aligned}
&\|\nabla e_\phi^{n+1}\|_{L^2}^2 + \|e_{\boldsymbol{u}}^{n+1}\|_{L^2}^2 + \|e_{\boldsymbol{B}}^{n+1}\|_{L^2}^2 \\
&\quad + \sum_{m=1}^{n}(\|\nabla \overline{e}_w^{n+\frac{1}{2}}\|_{L^2}^2 + \|\nabla \overline{e}_{\boldsymbol{u}}^{n+\frac{1}{2}}\|_{L^2}^2 + \|\nabla\times \overline{e}_{\boldsymbol{B}}^{n+\frac{1}{2}}\|_{L^2}^2 + \|\nabla\cdot \overline{e}_{\boldsymbol{B}}^{n+\frac{1}{2}}\|_{L^2}^2) \\
&\le C(h^{2r} + \tau^4).
\end{aligned} \tag{73}$$

An application of the triangle inequality, combined with projection estimates (42), (44) and (46), finally leads to the error estimates (29)–(30). This completes the proof of Theorem 3.1. □

5. Numerical examples

5.1. Convergence test

In this subsection we test the convergence order of the proposed numerical scheme. For simplicity, a two-dimensional domain $\Omega = (0, 2\pi)^2$ is taken and all the physical parameters are set to be 1, i.e $\varepsilon = \lambda = \sigma = \mu = 1$. The final time is given by $T = 0.5$. In addition, we adopt the linear element for p and the quadratic element for $\phi, w, \boldsymbol{u}, \boldsymbol{B}$. The exact solution is formulated as

$$\begin{aligned}
&\phi = -t^8 \cos x \cos y, \\
&w = -t^8 \cos x \cos y, \\
&\boldsymbol{u} = \begin{pmatrix} t^8 \sin^2 x \sin(2y) \\ -t^8 \sin(2x)\sin^2 y \end{pmatrix}, \\
&\boldsymbol{B} = \begin{pmatrix} -t^8 \sin y \cos x \\ t^8 \sin x \cos y \end{pmatrix}, \\
&p = t^8 \sin x \sin y.
\end{aligned} \tag{74}$$

We denote the numerical errors as

$$\begin{aligned}
&\mathcal{E}(\nabla\phi) = \|\nabla(\phi^N - \phi_h^N)\|_{L^2}, && \mathcal{E}(\boldsymbol{u}) = \|\boldsymbol{u}^N - \boldsymbol{u}_h^N\|_{L^2}, \\
&\mathcal{E}(\boldsymbol{B}) = \|\boldsymbol{B}^N - \boldsymbol{B}_h^N\|_{L^2}, && \mathcal{E}(\nabla w) = \textstyle\sum_{n=1}^{N-1} \|\nabla(\overline{w}^{n+\frac{1}{2}} - \overline{w}_h^{n+\frac{1}{2}})\|_{L^2}, \\
&\mathcal{E}(\nabla\boldsymbol{u}) = \textstyle\sum_{n=1}^{N-1} \|\nabla(\overline{\boldsymbol{u}}^{n+\frac{1}{2}} - \overline{\boldsymbol{u}}_h^{n+\frac{1}{2}})\|_{L^2}, && \mathcal{E}(\nabla\times\boldsymbol{B}) = \textstyle\sum_{n=1}^{N-1} \|\nabla\times(\overline{\boldsymbol{B}}^{n+\frac{1}{2}} - \overline{\boldsymbol{B}}_h^{n+\frac{1}{2}})\|_{L^2}.
\end{aligned}$$

To investigate the temporal convergence rate, we choose the spatial size h sufficiently small. For $h = 2\pi/120$ and $\tau = 1/18, 1/36, 1/54, 1/72$, the numerical errors between the exact solution and numerical solution generated by scheme (24)–(28) are displayed in Table 1. The numerical results demonstrate that the temporal convergence rate of the proposed scheme is of $\mathcal{O}(\tau^2)$, which is consistent with the theoretical analysis.

For the spatial convergence, we still adopt the exact solutions (74) and take the time step size as $\tau = 1/1200$ so that the temporal numerical error becomes negligible. The spatial mesh sizes are chosen as $h = 2\pi/20, 2\pi/40, 2\pi/60, 2\pi/80$ and the numerical results are displayed in Table 2. Clearly, the spatial convergence of ϕ and w in H^1 semi-norm is $\mathcal{O}(h^2)$, which is consistent with the theoretical results given in Theorem 3.1. From Table 2, the spatial convergence of $\boldsymbol{u}$ and $\boldsymbol{B}$ in L^2 norm is shown to be $\mathcal{O}(h^3)$ (one order higher than the theoretical results given in Theorem 3.1), which is still challenging to prove and its analysis will be considered in future works.

We also implement this numerical example by using the same time step sizes and spatial mesh sizes as above except for the parameter ε, for which we choose to be 0.1. Numerical results are shown in Tables 3 and 4, and the results indicate the order of accuracy as well.

Table 2
Spatial convergence for $\varepsilon = 1$ at $T = 0.5$.

h	$\mathcal{E}(\nabla\phi)$	Order	$\mathcal{E}(\boldsymbol{u})$	Order	$\mathcal{E}(\boldsymbol{B})$	Order
$2\pi/20$	1.665×10^{-4}		3.431×10^{-5}		8.168×10^{-6}	
$2\pi/40$	4.201×10^{-5}	1.99	4.560×10^{-6}	2.91	1.059×10^{-6}	2.95
$2\pi/60$	1.871×10^{-5}	1.99	1.390×10^{-6}	2.88	3.435×10^{-7}	2.78
$2\pi/80$	1.054×10^{-5}	1.99	6.062×10^{-7}	2.93	1.936×10^{-7}	1.99
h	$\mathcal{E}(\nabla w)$	Order	$\mathcal{E}(\nabla\boldsymbol{u})$	Order	$\mathcal{E}(\nabla\times\boldsymbol{B})$	Order
$2\pi/20$	2.859×10^{-5}		1.707×10^{-4}		2.815×10^{-5}	
$2\pi/40$	7.209×10^{-6}	1.99	4.350×10^{-5}	1.97	7.009×10^{-6}	2.01
$2\pi/60$	3.216×10^{-6}	1.99	1.940×10^{-5}	1.99	3.111×10^{-6}	2.00
$2\pi/80$	1.818×10^{-6}	1.98	1.093×10^{-5}	1.99	1.749×10^{-6}	2.00

Table 3
Temporal convergence for $\varepsilon = 0.1$ at $T = 0.5$.

τ	$\mathcal{E}(\nabla\phi)$	Order	$\mathcal{E}(\boldsymbol{u})$	Order	$\mathcal{E}(\boldsymbol{B})$	Order
1/18	9.749×10^{-4}		6.625×10^{-4}		6.169×10^{-4}	
1/36	2.831×10^{-4}	1.78	1.683×10^{-4}	1.98	1.561×10^{-4}	1.98
1/54	1.324×10^{-4}	1.87	7.504×10^{-5}	1.99	6.951×10^{-5}	2.00
1/72	7.646×10^{-5}	1.91	4.226×10^{-5}	2.00	3.913×10^{-5}	2.00
τ	$\mathcal{E}(\nabla w)$	Order	$\mathcal{E}(\nabla\boldsymbol{u})$	Order	$\mathcal{E}(\nabla\times\boldsymbol{B})$	Order
1/18	6.431×10^{-3}		3.025×10^{-4}		1.712×10^{-4}	
1/36	2.145×10^{-3}	1.58	7.627×10^{-5}	1.99	4.288×10^{-5}	2.00
1/54	1.040×10^{-3}	1.79	3.422×10^{-5}	1.98	1.907×10^{-5}	2.00
1/72	6.101×10^{-4}	1.85	1.967×10^{-5}	1.92	1.075×10^{-5}	1.99

Table 4
Spatial convergence for $\varepsilon = 0.1$ at $T = 0.5$.

h	$\mathcal{E}(\nabla\phi)$	Order	$\mathcal{E}(\boldsymbol{u})$	Order	$\mathcal{E}(\boldsymbol{B})$	Order
$2\pi/20$	1.745×10^{-4}		3.431×10^{-5}		8.168×10^{-6}	
$2\pi/40$	4.216×10^{-5}	2.05	4.596×10^{-6}	2.90	1.059×10^{-6}	2.95
$2\pi/60$	1.873×10^{-5}	2.00	1.390×10^{-6}	2.95	3.435×10^{-7}	2.78
$2\pi/80$	1.054×10^{-5}	2.00	6.062×10^{-7}	2.88	1.936×10^{-7}	1.99
h	$\mathcal{E}(\nabla w)$	Order	$\mathcal{E}(\nabla\boldsymbol{u})$	Order	$\mathcal{E}(\nabla\times\boldsymbol{B})$	Order
$2\pi/20$	4.410×10^{-5}		1.707×10^{-4}		2.815×10^{-5}	
$2\pi/40$	7.967×10^{-6}	2.47	4.350×10^{-5}	1.97	7.009×10^{-6}	2.01
$2\pi/60$	4.071×10^{-6}	1.66	1.940×10^{-5}	1.99	3.111×10^{-6}	2.00
$2\pi/80$	3.054×10^{-6}	1.00	1.093×10^{-5}	1.99	1.749×10^{-6}	2.00

5.2. Energy stability test

In this subsection we investigate the energy dissipation property of the numerical scheme (24)–(28). Similarly, the quadratic element is adopted for ϕ, w, $\boldsymbol{u}$, $\boldsymbol{B}$, and the linear element is used for p. The spatial resolution and the time step size are taken as $h = 2\pi/20$ and $\tau = 0.1$, respectively. The initial data are set to be

$$\begin{aligned}
\phi_0 &= -\cos x \cos y,\\
w_0 &= -\cos x \cos y,\\
\boldsymbol{u}_0 &= \begin{pmatrix} \sin^2 x \sin(2y) \\ -\sin(2x)\sin^2 y \end{pmatrix},\\
\boldsymbol{B}_0 &= \begin{pmatrix} -\sin y \cos x \\ \sin x \cos y \end{pmatrix},\\
p_0 &= \sin x \sin y.
\end{aligned} \tag{75}$$

Then we compute the discrete energy (33) up to final time $T = 10$, and the energy evolution curve is displayed in Fig. 1, where the dissipation for the discrete energy (33) could be clearly observed.

6. Conclusion

In this paper, we propose and analyze a temporally second-order accurate, mixed finite element numerical method for the Cahn–Hilliard-Magnetohydrodynamic system (6)–(10). The primary difficulties are associated with the coupled nature

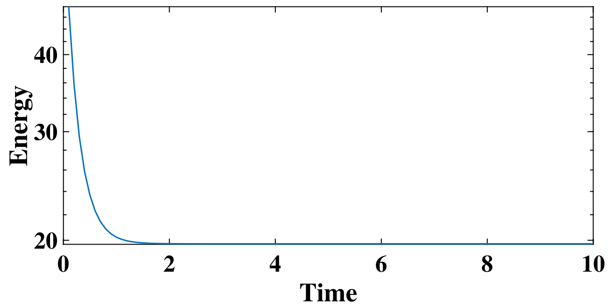

Fig. 1. Discrete energy evolution of numerical solutions for the CH-MHD system.

of the fluid motion, electric field, and phase evolution. The nonlinearity of the free energy in the phase field makes the system even more challenging. In the proposed numerical scheme, a modified Crank–Nicolson approximation is applied to the phase field and the free energy, combined with a second-order explicit extrapolation for the concave part. Such a numerical approximation ensures energy stability and unique solvability for the phase field. In addition, second-order semi-implicit treatments are used for other coupled parts in the system. As a result, the discrete mass conservation, unique solvability, and energy stability have been theoretically established for the numerical scheme. The error estimates have been also derived, in the $L^\infty_\tau(0, T; H^1)$ norm for the phase variable, and $L^\infty_\tau(0, T; L^2)$ norm for the velocity and magnetic variables. Several numerical examples are presented to demonstrate the robustness and accuracy of the proposed scheme. The numerical simulations and corresponding theoretical analyses of the Cahn–Hilliard-Magnetohydrodynamics model with $\varepsilon \ll 1$ and $\mu \ll 1$ are challenging and interesting, and will be considered in future works.

Data availability

No data was used for the research described in the article.

Acknowledgments

The authors would like to thank the anonymous referees for their valuable comments and suggestions. The research of C. Wang was supported in part by NSF DMS-2012269. The research of J. Wang was supported in part by NSFC-12071020 and NSFC-12131005. The research of S. M. Wise was supported in part by NSF DMS-1719854 and DMS-2012634. The research of Z. Xia was supported in part by NSFC-11871139. The research of L. Xu was supported in part by NSFC-12071060.

References

[1] J. Yang, S. Mao, X. He, X. Yang, Y. He, A diffuse interface model and semi-implicit energy stable finite element method for two-phase magnetohydrodynamic flows, Comput. Methods Appl. Mech. Engrg. 356 (2019) 435–464.
[2] X. Feng, Fully discrete finite element approximations of the Navier–Stokes–cahn–hilliard diffuse interface model for two-phase fluid flows, SIAM J. Numer. Anal. 44 (3) (2006) 1049–1072.
[3] D. Jacqmin, Calculation of two-phase Navier–Stokes flows using phase-field modeling, J. Comput. Phys. 155 (1) (1999) 96–127.
[4] R. Chen, H. Zhang, Second-order energy stable schemes for the new model of the cahn-hilliard-MHD equations, Adv. Comput. Math. 46 (6) (2020) No. 79, 28.
[5] J. Zhao, R. Chen, H. Su, An energy-stable finite element method for incompressible magnetohydrodynamic–Cahn–Hilliard coupled model, Adv. Appl. Math. Mech. 13 (4) (2021) 761–790.
[6] H. Su, G.-D. Zhang, Highly efficient and energy stable schemes for the 2D/3D diffuse interface model of two-phase magnetohydrodynamics, J. Sci. Comput. 90 (1) (2022) Paper No. 63, 31.
[7] S. Asai, Magnetohydrodynamics in Materials Processing, Springer Netherlands, 2012.
[8] Y. Unger, M. Mond, H. Branover, Liquid Metal Flows: Magnetohydrodynamics and Application, American Institute of Astronautics and Aeronautics, 1988.
[9] J.A. Shercliff, A Textbook of Magnetohydrodyamics, Pergamon Press, Oxford-New York-Paris, 1965.
[10] C. He, Y. Wang, On the regularity criteria for weak solutions to the magnetohydrodynamic equations, J. Differential Equations 238 (1) (2007) 1–17.
[11] F. Lin, L. Xu, P. Zhang, Global small solutions of 2-D incompressible MHD system, J. Differ. Equ. 259 (10) (2015) 5440–5485.
[12] F. Lin, P. Zhang, Global small solutions to an MHD-type system: The three-dimensional case, Commun. Pure Appl. Anal. 67 (4) (2014) 531–580.
[13] M.E. Schonbek, T.P. Schonbek, E. Süli, Large-time behaviour of solutions to the magnetohydrodynamics equations, Math. Ann. 304 (4) (1996) 717–756.
[14] L. Xu, P. Zhang, Global small solutions to three-dimensional incompressible magnetohydrodynamical system, SIAM J. Math. Anal. 47 (1) (2015) 26–65.
[15] M.D. Gunzburger, A.J. Meir, J.S. Peterson, On the existence, uniqueness, and finite element approximation of solutions of the equations of stationary, incompressible magnetohydrodynamics, Math. Comp. 56 (194) (1991) 523–563.

[16] Y. He, Unconditional convergence of the Euler semi-implicit scheme for the three-dimensional incompressible MHD equations, IMA J. Numer. Anal. 35 (2) (2015) 767–801.
[17] J.-F. Gerbeau, A stabilized finite element method for the incompressible magnetohydrodynamic equations, Numer. Math. 87 (1) (2000) 83–111.
[18] J.L. Guermond, P.D. Minev, Mixed finite element approximation of an MHD problem involving conducting and insulating regions: the 3D case, Numer. Methods Partial Differential Equations 19 (6) (2003) 709–731.
[19] Y. He, J. Zou, A priori estimates and optimal finite element approximation of the MHD flow in smooth domains, M2AN Math. Model. Numer. Anal. 52 (1) (2018) 181–206.
[20] B. Li, J. Wang, L. Xu, A convergent linearized Lagrange finite element method for the magneto-hydrodynamic equations in two-dimensional nonsmooth and nonconvex domains, SIAM J. Numer. Anal. 58 (1) (2020) 430–459.
[21] X. Yang, G.-D. Zhang, X. He, Convergence analysis of an unconditionally energy stable projection scheme for magneto-hydrodynamic equations, Appl. Numer. Math. 136 (2019) 235–256.
[22] G.-D. Zhang, X. He, X. Yang, A decoupled, linear and unconditionally energy stable scheme with finite element discretizations for magneto-hydrodynamic equations, J. Sci. Comput. 81 (3) (2019) 1678–1711.
[23] H. Gao, W. Qiu, A semi-implicit energy conserving finite element method for the dynamical incompressible magnetohydrodynamics equations, Comput. Methods Appl. Mech. Engrg. 346 (2019) 982–1001.
[24] A. Prohl, Convergent finite element discretizations of the nonstationary incompressible magnetohydrodynamics system, M2AN Math. Model. Numer. Anal. 42 (6) (2008) 1065–1087.
[25] J. Ridder, Convergence of a finite difference scheme for two-dimensional incompressible magnetohydrodynamics, SIAM J. Numer. Anal. 54 (6) (2016) 3550–3576.
[26] T. Heister, M. Mohebujjaman, L.G. Rebholz, Decoupled, unconditionally stable, higher order discretizations for MHD flow simulation, J. Sci. Comput. 71 (1) (2017) 21–43.
[27] W. Layton, H. Tran, C. Trenchea, Numerical analysis of two partitioned methods or uncoupling evolutionary MHD flows, Numer. Methods Partial Differ. Equ. 30 (4) (2014) 1083–1102.
[28] G.-D. Zhang, X. He, X. Yang, A fully decoupled linearized finite element method with second-order temporal accuracy and unconditional energy stability for incompressible MHD equations, J. Comput. Phys. 448 (2022) Paper No. 110752, 19.
[29] R. Hiptmair, L. Li, S. Mao, W. Zheng, A fully divergence-free finite element method for magnetohydrodynamic equations, Math. Models Methods Appl. Sci. 28 (4) (2018) 659–695.
[30] C. Wang, J. Wang, Z. Xia, L. Xu, Optimal error estimates of a Crank–Nicolson finite element projection method for magnetohydrodynamic equations, M2AN Math. Model. Numer. Anal. 56 (3) (2022) 767–789.
[31] S.M. Allen, J.W. Cahn, A microscopic theory for antiphase boundary motion and its application to antiphase domain coarsening, Acta. Metall. 27 (1979) 1085.
[32] J.W. Cahn, J.E. Hilliard, Free energy of a nonuniform system. I. Interfacial free energy, J. Chem. Phys. 28 (1958) 258–267.
[33] A.E. Diegel, C. Wang, S.M. Wise, Stability and convergence of a second-order mixed finite element method for the Cahn–Hilliard equation, IMA J. Numer. Anal. 36 (4) (2016) 1867–1897.
[34] J. Guo, C. Wang, S.M. Wise, X. Yue, An H^2 convergence of a second-order convex-splitting, finite difference scheme for the three-dimensional Cahn–Hilliard equation, Commun. Math. Sci. 14 (2) (2016) 489–515.
[35] J. Guo, C. Wang, S.M. Wise, X. Yue, An improved error analysis for a second-order numerical scheme for the Cahn–Hilliard equation, J. Comput. Appl. Math. 388 (113300) (2021) 16.
[36] A.E. Diegel, X. Feng, S.M. Wise, Analysis of a mixed finite element method for a cahn–hilliard–Darcy–Stokes system, SIAM J. Numer. Anal. 53 (1) (2015) 127–152.
[37] A.E. Diegel, C. Wang, X. Wang, S.M. Wise, Convergence analysis and error estimates for a second order accurate finite element method for the Cahn–Hilliard–Navier–Stokes system, Numer. Math. 137 (3) (2017) 495–534.
[38] D. Han, X. Wang, A second order in time, uniquely solvable, unconditionally stable numerical scheme for Cahn–Hilliard–Navier–Stokes equation, J. Comput. Phys. 290 (2015) 139–156.
[39] J. Shen, X. Yang, Decoupled, energy stable schemes for phase-field models of two-phase incompressible flows, SIAM J. Numer. Anal. 53 (1) (2015) 279–296.
[40] W. Chen, Y. Liu, C. Wang, S.M. Wise, Convergence analysis of a fully discrete finite difference scheme for the Cahn–Hilliard–Hele–Shaw equation, Math. Comp. 85 (301) (2016) 2231–2257.
[41] W. Chen, S. Wang, Y. Zhang, D. Han, C. Wang, X. Wang, Error estimate of a decoupled numerical scheme for the cahn–hilliard–Stokes–Darcy system, IMA J. Numer. Anal. 42 (3) (2022) 2621–2655.
[42] Y. Chen, J. Shen, Efficient, adaptive energy stable schemes for the incompressible cahn–hilliard Navier–Stokes phase-field models, J. Comput. Phys. 308 (2016) 40–56.
[43] X. Feng, Y. He, C. Liu, Analysis of finite element approximations of a phase field model for two-phase fluids, Math. Comp. 76 (258) (2007) 539–571.
[44] X. Feng, S.M. Wise, Analysis of a Darcy–Cahn–Hilliard diffuse interface model for the Hele–Shaw flow and its fully discrete finite element approximation, SIAM J. Numer. Anal. 50 (3) (2012) 1320–1343.
[45] J. Shen, X. Yang, A phase-field model and its numerical approximation for two-phase incompressible flows with different densities and viscosities, SIAM J. Sci. Comput. 32 (3) (2010) 1159–1179.
[46] J. Zhang, X. Yang, Efficient and accurate numerical scheme for a magnetic-coupled phase-field-crystal model for ferromagnetic solid materials, Comput. Methods Appl. Mech. Engrg. 371 (2020) 113310, 20.
[47] J. Zhang, X. Yang, A new magnetic-coupled cahn-hilliard phase-field model for diblock copolymers and its numerical approximations, Appl. Math. Lett. 107 (2020) 106412, 9.
[48] J. Shen, X. Yang, The IEQ and SAV approaches and their extensions for a class of highly nonlinear gradient flow systems, in: 75 Years of Mathematics of Computation, in: Contemp. Math., vol. 754, Amer. Math. Soc., [Providence], RI, 2020, pp. 217–245, ©[2020].
[49] X. Yang, Linear, first and second-order, unconditionally energy stable numerical schemes for the phase field model of homopolymer blends, J. Comput. Phys. 327 (2016) 294–316.
[50] Z. Si, J. Wang, W. Sun, Unconditional stability and error estimates of modified characteristics FEMs for the Navier-Stokes equations, Numer. Math. 134 (1) (2016) 139–161.
[51] S.C. Brenner, L.R. Scott, The Mathematical Theory of Finite Element Methods, third ed., in: Texts in Applied Mathematics, vol. 15, Springer, New York, 2008.
[52] V. Girault, P. Raviart, Finite Element Method for Navier–Stokes Equations: Theory and Algorithms, Springer-Verlag, Berlin, Herdelberg, 1987.
[53] V. Thomée, Galerkin Finite Element Methods for Parabolic Problems, Springer-Verlag, Berlin, 2006.